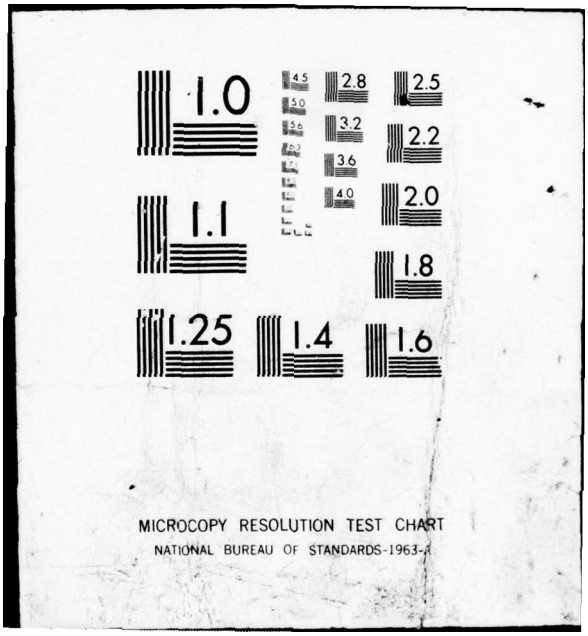
AD-A054 759 DOUGLAS AIRCRAFT CO LONG BEACH CALIF F/G 20/4
BOUNDARY-LAYER AND INVERSE POTENTIAL-FLOW METHODS FOR AXISYMMET--ETC(U)
MAR 78 T CEBECI , K KAUPS, R M JAMES N00014-77-C-0087
UNCLASSIFIED MDC-J7895 NL

| OF |
AD
A054759



END
DATE
FILMED
7-78
DDC


1.0
1.1
1.25
1.4
1.6
1.8
2.0
2.2
2.5
2.8
3.2
3.6
4.0
4.5
5.0
5.6
MICROCOPY RESOLUTION TEST CHART
NATIONAL BUREAU OF STANDARDS-1963-A

AD A054759

112

REPORT NO. MDC J7895

BOUNDARY-LAYER AND INVERSE POTENTIAL-FLOW METHODS FOR AXISYMMETRIC BODIES

BY

TUNCER CEBECI, KALLE KAUPS, R. M. JAMES AND D. P. MACK

MARCH 1978

prepared under
contract N00014-77-C-0057
FOR
OFFICE OF NAVAL RESEARCH
800 QUINCY STREET
ARLINGTON, VIRGINIA 22217

DDC
RECEIVED
JUN 7 1978
F

This document has been approved for public release and sale; its distribution is unlimited.

DOUGLAS AIRCRAFT COMPANY

MCDONNELL DOUGLAS CORPORATION

Copy number

Report number MDC J7895

BOUNDARY-LAYER AND INVERSE POTENTIAL-FLOW METHODS FOR AXISYMMETRIC BODIES

Revision date

Revision letter

Issue date March 1978

Contract number N00014-77-C-0087

Prepared by : Tuncer Cebeci, Kalle Kaups, R. M. James and D. P. Mack

Approved by :

F. T. Lynch
Chief Aerodynamics Engineer
Research & Development Programs

R. B. Harris
Chief Technology Engineer
Aerodynamics

DOUGLAS AIRCRAFT COMPANY
MCDONNELL DOUGLAS CORPORATION

Preceding Page BLANK - FILMED

TABLE OF CONTENTS

		Page
1.0	Introduction	1
2.0	Boundary-Layer Method	2
2.1	Boundary-Layer Equations	2
2.2	Fluid Properties	3
2.3	Turbulence Model	5
2.4	Mangler-Falkner-Skan Transformation	6
2.5	Solution Procedure	8
2.6	Boundary-Layer Parameters	9
3.0	Description of the Boundary-Layer Computer Program	11
3.1	Input	11
3.2	Output	15
3.3	Sample Calculations	18
4.0	Standard and Inverse Potential-Flow Method	35
4.1	Equations of Motion	35
4.2	Unit Circle Mapping	36
4.3	Method of Solution	38
4.4	Boundary Conditions	40
4.5	Velocity Calculation	42
4.6	Solution Procedure	43
5.0	Description of the Potential-Flow Computer Program	45
5.1	Input	45
5.2	Output	47
5.3	Sample Calculations	48
6.0	References	54

ACCESSION for
NTIS White Section
DDC Buff Section
UNANNOUNCED
JUSTIFICATION
BY
DISTRIBUTION/AVAILABILITY CODES
Dist. SPECIAL
A

Unclassified

SECURITY CLASSIFICATION OF THIS PAGE (When Data Entered)

REPORT DOCUMENTATION PAGE

READ INSTRUCTIONS BEFORE COMPLETING FORM

1. REPORT NUMBER

2. GOVT ACCESSION NO.

3. RECIPIENT'S CATALOG NUMBER

4. TITLE (and Subtitle)
Boundary-Layer and Inverse Potential-Flow Methods for Axisymmetric Bodies.

5. TYPE OF REPORT & PERIOD COVERED
Final Technical rept.
January 1977 — March 1978

6. PERFORMING ORG. REPORT NUMBER
MDC-J7895

7. AUTHOR(s)
Tuncer Cebeci, Kalle Kaups, R. M. James, and D. P. Mack

8. CONTRACT OR GRANT NUMBER(s)
N00014-77-C-0087 new

9. PERFORMING ORGANIZATION NAME AND ADDRESS
Douglas Aircraft Company
3855 Lakewood Boulevard
Long Beach, California 90846

10. PROGRAM ELEMENT, PROJECT, TASK AREA & WORK UNIT NUMBERS

11. CONTROLLING OFFICE NAME AND ADDRESS
Office of Naval Research, Dept. of the Navy
800 Quincy Street
Arlington, Virginia 22217

12. REPORT DATE
March 1978

13. NUMBER OF PAGES
56

14. MONITORING AGENCY NAME & ADDRESS (if different from Controlling Office)
12 59p.

15. SECURITY CLASS. (of this report)
Unclassified

15a. DECLASSIFICATION/DOWNGRADING SCHEDULE

16. DISTRIBUTION STATEMENT (of this Report)

Distribution unlimited

17. DISTRIBUTION STATEMENT (of the abstract entered in Block 20, if different from Report)

18. SUPPLEMENTARY NOTES

19. KEY WORDS (Continue on reverse side if necessary and identify by block number)

Laminar and turbulent boundary layers
Axisymmetric flows
Inviscid flows

20. ABSTRACT (Continue on reverse side if necessary and identify by block number)

This report provides a description of two methods and their computer programs for calculating viscous and inviscid flows past axisymmetric bodies. The first is a boundary-layer method for both laminar and turbulent flows. The procedure embodies a finite-difference representation of the boundary-layer equations and uses an eddy-viscosity model to represent turbulent flows.

The second method is an inviscid-flow procedure which obtains solutions to the potential equation by an orthogonal expansion procedure. The accuracy

DD FORM 1 JAN 73 1473 EDITION OF 1 NOV 65 IS OBSOLETE
S/N 0102-014-6601

Unclassified

SECURITY CLASSIFICATION OF THIS PAGE (When Data Entered)

116 400

is equivalent to higher-order Neumann solutions, but at a considerable savings of computer time. This method can be used in either a direct or an inverse mode.

Details of each method are presented and the use of the computer program is documented with various test cases.

1.0 INTRODUCTION

This report provides a description of two methods and their computer programs for calculating viscous and inviscid flows past axisymmetric bodies. The first is a boundary-layer method for both laminar and turbulent flows. The procedure embodies a finite-difference representation of the boundary-layer equations and uses an eddy-viscosity model to represent turbulent flows. The details of the eddy-viscosity model and an indication of its range of applicability for flows past surfaces with heat and mass transfer is provided by Cebeci and Smith[1]. The two-point finite-difference method is described by Cebeci and Bradshaw[2]. Section 2 describes the method and states the boundary-layer equations, corresponding boundary conditions, fluid properties, turbulence model, solution procedure and the boundary-layer parameters. Section 3 describes the computer program and states the input and output of the computer program together with three sample calculations to demonstrate the capability and use of the computer program.

The second method is an inviscid-flow procedure developed by James[3]. Solutions to the potential equation are obtained by an orthogonal expansion procedure. For the cases to be presented, the accuracy is equivalent to higher-order Neumann solutions, but at a considerable savings of computer time. When used in the direct mode, this computer code yields the pressure distribution (edge velocities for boundary-layer calculations) for any specified body shape. An additional feature of the inviscid procedure is its capability to be used in an inverse (or design) mode. Here, the desired velocity on the body is specified, and the procedure will yield the body shape consistent with this velocity. Details of the development of the method are given in Section 4. Section 5 describes the use of the computer program, and demonstrates its capabilities on five different body shapes.

2.0 BOUNDARY-LAYER METHOD

2.1 Boundary-Layer Equations

The governing boundary-layer equations for steady axisymmetric compressible laminar and turbulent boundary layers are the continuity, momentum, and energy equations. These equations and their boundary conditions for the coordinate system shown in figure 1 are:

Continuity

$$\frac{\partial}{\partial x}(\rho u r) + \frac{\partial}{\partial y}(\overline{\rho} v r) = 0 \tag{2.1}$$

Momentum

$$\rho u \frac{\partial u}{\partial x} + \overline{\rho v} \frac{\partial u}{\partial y} = u_e \frac{du_e}{dx} + \frac{1}{r}\frac{\partial}{\partial y}\left[r\left(\mu \frac{\partial u}{\partial y} - \rho\overline{u'v'}\right)\right] \tag{2.2}$$

Energy

$$\rho u \frac{\partial H}{\partial x} + \overline{\rho v} \frac{\partial H}{\partial y} = \frac{1}{r}\frac{\partial}{\partial y}\left\{r\left[\frac{\mu}{Pr}\frac{\partial H}{\partial y} - \rho\overline{v'H'} + \mu\left(1 - \frac{1}{Pr}\right) u \frac{\partial u}{\partial y}\right]\right\} \tag{2.3}$$

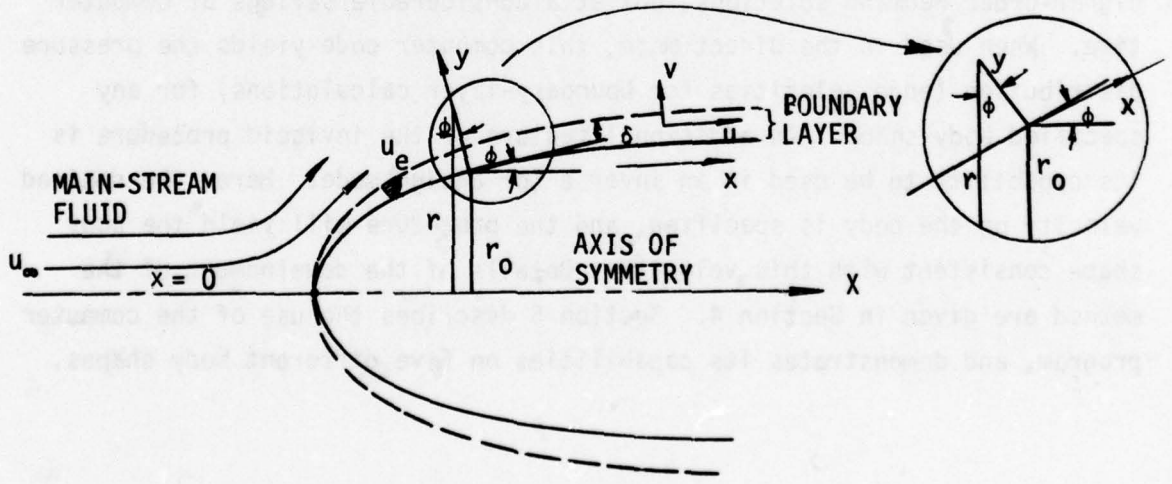


Figure 1. The notation and the coordinate system for axisymmetric flows.

$$y = 0 \qquad u = 0, \qquad v = v_w(x), \qquad H = H_w \quad \text{or} \quad \left(\frac{\partial H}{\partial y}\right)_w = \text{given} \tag{2.4a}$$

$$y \to \infty \qquad u \to u_e(x), \qquad H \to H_e \tag{2.4b}$$

Here

$$\overline{\rho v} = \rho v + \overline{\rho' v'}$$

$$r = r_o + y \cos\phi \tag{2.5a}$$

$$\phi = \tan^{-1} \frac{dr_o}{dx} \tag{2.5b}$$

We note that with r being a function of x and y, these equations account for the transverse curvature effect which becomes important when the boundary-layer thickness is of the same order of magnitude as the body radius r_o.

The solution of the system given by (2.1) - (2.4) requires fluid properties and closure assumptions for the Reynolds stresses, $-\rho\overline{u'v'}$ and $-\rho\overline{v'H'}$. In this report we consider both air and water and discuss their fluid properties in Section 2.2. To satisfy the closure assumptions, we use the eddy-diffusivity concept and represent them by the algebraic eddy viscosity formulation of Cebeci and Smith[1]. The relevant equations for the eddy-viscosity formulas are discussed in Section 2.3.

2.2 Fluid Properties

The solution of the boundary-layer equations require the specification of fluid properties. In our study we consider air, pure water and sea water as the working fluid and define their properties below. Air is treated as a perfect gas, and the fluid properties μ and ρ are assumed to be functions of temperature only. The specific heat of air at constant pressure, namely, C_p, is assumed to be constant and equal to 6006 $ft^2/sec^2{}^\circ R$. The viscosity is obtained from Sutherland's law expressed as

$$\mu = 2.270 \times 10^{-8} \frac{T^{3/2}}{T + 198.6} \quad \frac{lb_f\text{-sec}}{ft^2} \tag{2.6}$$

The density-temperature relation is obtained from the equation of state and from the assumption that the static pressure remains constant within the boundary layer,

$$\rho = \frac{Pe}{1716T} \frac{lb_f\text{-sec}^2}{ft^2} \tag{2.7}$$

The Prandtl number of air is an input to the computer program and is assumed to be constant.

The fluid properties of <u>pure water</u> are given by:

$$\mu = 3.74614 \times 10^{-5} / (35.155539 - 106.9718715T_r + 107.7720376T_r^2 - 40.5953074T_r^3 + 5.6391948T_r^4) \tag{2.8}$$

$$\rho = 1.94 (0.803928 + 0.4615901T_r - 0.2869774T_r^2 + 0.0234689T_r^3) \tag{2.9}$$

$$c_p = 25222.98 (1.4833689 - 0.8072501T_r + 0.3289607T_r^2) \tag{2.10}$$

$$Pr = 13.66 / (73.376906 - 208.7474538T_r + 197.7604676T_r^2 - 68.8626188T_r^3 + 7.4779458T_r^4) \tag{2.11}$$

$$k = 6.917333 \times 10^{-2} (-1.9410583 + 5.2220185T_r - 2.693322T_r^2 + 0.4176176T_r^3) \tag{2.12}$$

The fluid properties of <u>sea water</u> are given by:

$$\mu = 3.9258 \times 10^{-5} / (-289.99547 + 1101.820526T_r - 1577.2442T_r^2 + 1003.8069T_r^3 - 237.3881T_r^4) \tag{2.13}$$

$$\rho = 1.9947 (0.66285108 + 0.69246952T_r - 0.3553206T_r^2) \tag{2.14}$$

$$c_p = 23859.32 (1.774152 - 1.518056T_r + 0.7439018T_r^2) \tag{2.15}$$

$$Pr = 13.565 / (-686.60487 + 2653.55416T_r - 3851.34007T_r^2 + 2482.21458T_r^3 - 596.8245T_r^4) \tag{2.16}$$

$$k = 6.90492 \times 10^{-2} (12.28011 - 35.655012T_r + 36.562345T_r^2 - 12.187448T_r^3) \tag{2.17}$$

Here T_r is a temprature ratio defined by

$$Tr = \frac{T}{491.69} \tag{2.18}$$

The units of μ, ρ, c_p, k and T in (2.8) - (2.17) are lb_f-sec/ft^2, slugs/ft^3, ft^2/sec°R, (lb_f-ft)/sec ft°R, °R, respectively.

2.3 Turbulence Model

To satisfy the closure conditions we use the eddy viscosity (ε_m) and eddy-conductivity (ε_H) concepts and define them by

$$-\rho\overline{u'v'} = \rho\varepsilon_m \frac{\partial u}{\partial y}, \qquad -\rho\overline{v'H'} = \rho\varepsilon_H \frac{\partial H}{\partial y} \tag{2.19}$$

and relate ε_m and ε_H to a turbulent Prandtl number Pr_t by

$$Pr_t = \frac{\varepsilon_m}{\varepsilon_H} \tag{2.20}$$

According to the eddy-viscosity formulation of Cebeci and Smith[1], the turbulent boundary layer is divided into two regions, called inner and outer regions, and eddy-viscosity formulas are defined by separate formulas in each region. They are:

$$\varepsilon_m = \begin{cases} (\varepsilon_m)_i = L^2 \left|\frac{\partial u}{\partial y}\right| \gamma_{tr} & (\varepsilon_m)_i \le (\varepsilon_m)_o \quad (2.21a) \\ (\varepsilon_m)_o = 0.0168 \left|\int_0^\infty (u_e - u)dy\right| \gamma_{tr} & (\varepsilon_m)_o > (\varepsilon_m)_i \quad (2.21b) \end{cases}$$

Here

$$L = 0.4y[1 - \exp(-y/A)] \tag{2.22a}$$

$$A = 26\nu/N\, u_\tau^{-1} (\rho/\rho_w)^{1/2}, \qquad u_\tau = (\tau_w/\rho_w)^{1/2} \tag{2.22b}$$

For flows with no mass transfer the parameter N is

$$N = \left[1 - 11.8 \left(\frac{\mu_w}{\mu_e}\right)\left(\frac{\rho_e}{\rho_w}\right)^2 p^+\right]^{1/2} \tag{2.22c}$$

When there is mass transfer

$$N = \left\{\frac{\mu}{\mu_e}\left(\frac{\rho_e}{\rho_w}\right)^2 \frac{p^+}{v_w^+}\left[1 - \exp\left(11.8 \frac{\mu_w}{\mu} v_w^+\right)\right] + \exp\left(11.8 \frac{\mu_w}{\mu} v_w^+\right)\right\}^{1/2} \tag{2.22d}$$

where

$$p^+ = \frac{\nu_e u_e}{u_\tau^3}\frac{du_e}{dx}, \qquad v_w^+ = \frac{v_w}{u_\tau} \tag{2.22e}$$

The parameter γ_{tr} allows for the finite length of the transitional region between a laminar and a turbulent flow and is given by

$$\gamma_{tr} = 1 - \exp\left[-G(r_o)_{tr}\left(\int_{x_{tr}}^{x}\frac{dx}{r_o(x)}\right)\left(\int_{x_{tr}}^{x}\frac{dx}{u_e}\right)\right] \tag{2.22f}$$

Here G is a spot-formation-rate parameter

$$G = \frac{1}{1200}\left(\frac{u_e^3}{\nu_e^2}\right)R_{x_{tr}}^{-1.34}, \qquad R_{x_{tr}} = \left(\frac{u_e x}{\nu_e}\right)_{tr} \tag{2.22g}$$

According to the studies conducted by Cebeci and Smith, a constant value of turbulent Prandtl number is quite satisfactory for the type of flows to be considered in this study. Therefore, we assume $Pr_t = 0.90$.

2.4 Mangler-Falkner-Skan Transformation

Before we solve the boundary-layer equations for both laminar and turbulent flows, we use a combination of Mangler and Falkner-Skan transformation. For this purpose we define new independent variables $\bar{x}$ and η by

$$d\bar{x} = \left(\frac{r_o}{L}\right)^2 dx \tag{2.23a}$$

$$d\eta = \left(\frac{u_e}{\rho_e \mu_e \bar{x}}\right)^{1/2}\rho\left(\frac{r}{L}\right)dy \tag{2.23b}$$

and by introducing a stream function that satisfies the continuity equation (2.1)

$$\psi = (\rho_e \mu_e u_e \bar{x})^{1/2} L f(x,\eta) \tag{2.23c}$$

so that

$$\rho u r = \frac{\partial \psi}{\partial y}, \qquad \overline{\rho v r} = -\frac{\partial \psi}{\partial x} + \rho_w v_w r_o \tag{2.24}$$

With this transformation it can be shown that the momentum and energy equations and their boundary conditions can be written as

Momentum

$$(b_1 f'')' + m_1 f f'' + m_2[c - (f')^2] - m_3 f'' = \bar{x}\left(f' \frac{\partial f'}{\partial \bar{x}} - f'' \frac{\partial f}{\partial \bar{x}}\right) \quad (2.25)$$

Energy

$$(b_3 E')' + (b_2 f' f'')' + (m_1 f - m_3)E' = \bar{x}\left(f' \frac{\partial E}{\partial \bar{x}} - E' \frac{\partial f}{\partial \bar{x}}\right) \quad (2.26)$$

$$\eta = 0 \qquad f = f' = 0 \qquad \tilde{\alpha}_o E_w + \tilde{\alpha}_1 E_w' = \text{given} \quad (2.27a)$$

$$\eta \to \eta_\infty \qquad f' \to 1 \qquad E \to 1 \quad (2.27b)$$

Here primes denote differentiation with respect to η and

$$\left.\begin{aligned} b_1 &= C(1+t)^2(1+\varepsilon_m^+), \quad C = \frac{\rho\mu}{\rho_e \mu_e}, \quad c = \frac{\rho_e}{\rho}, \quad \varepsilon_m^+ = \frac{\varepsilon_m}{\nu} \\ b_2 &= C\left(1 - \frac{1}{Pr}\right)\frac{u_e^2}{H_e}, \qquad b_3 = \frac{C}{Pr}(1+t)^2\left(1 + \frac{Pr}{Pr_t}\varepsilon_m^+\right) \end{aligned}\right\} \quad (2.28)$$

$$\left.\begin{aligned} m_1 &= \frac{1}{2}\left[1 + m_2 + \frac{\bar{x}}{\rho_e \mu_e}\frac{d}{d\bar{x}}(\rho_e \mu_e)\right], \qquad m_2 = \frac{\bar{x}}{u_e}\frac{du_e}{d\bar{x}}, \\ m_3 &= \frac{\rho_w v_w}{\rho_e u_e} R_{\bar{x}}^{1/2}\left(\frac{L}{r_o}\right), \qquad R_{\bar{x}} = \frac{u_e \bar{x}}{\nu_e} \\ t &= -1 + \left[1 + \frac{2(\bar{x}/L)\cos\phi I_1}{(r_o/L)^2 (R_{\bar{x}})^{1/2}}\right]^{1/2}, \qquad I_1 = \int_0^\eta c\, d\eta \end{aligned}\right\} \quad (2.29)$$

$$f' = \frac{u}{u_e}, \qquad E = \frac{H}{H_e} \quad (2.30)$$

Similarly the eddy-viscosity formulas given in Section 2.3 can be expressed in transformed variables and can be written as

$$(\varepsilon_m^+)_i = 0.16\, C^2 \left(\frac{\mu_e}{\mu}\right)^3 \left(\frac{r_o}{L}\right)^3 \left(\frac{L}{\bar{x}}\right)^2 R_{\bar{x}}^{3/2} \frac{(1+t)t^2}{\cos^2\phi}\left[1 - \exp\left(-\frac{t}{\cos\phi}\frac{r_o}{A}\right)\right]^2 |f''|\gamma_{tr} \quad (2.31a)$$

$$(\varepsilon_m^+)_o = 0.0168C \left(\frac{\mu_e}{\mu}\right)^2 \left(\frac{L}{r_o}\right) R_{\bar{x}}^{1/2} \left| \int_0^{\eta_\infty} \frac{c(1 - f')}{(1 + t)} \, d\eta \right|_{\gamma_{tr}} \tag{2.31b}$$

Here

$$\frac{r_o}{A} = \frac{N}{26} R_{\bar{x}}^{3/4} \left(\frac{r_o}{L}\right)^{3/2} \left(\frac{L}{\bar{x}}\right) c^{-3/2} \frac{C_w^{1/2}}{C} (f_w'')^{1/2} \tag{2.32a}$$

$$p^+ = \frac{\nu_e}{u_\tau^3} u_e \frac{du_e}{d\bar{x}}, \qquad u_\tau = u_e \left[\left(\frac{\mu_w}{\mu_e}\right)\left(\frac{r_o}{L}\right) R_{\bar{x}}^{-1/2} (f_w'')\right]^{1/2} \tag{2.32b}$$

2.5 Solution Procedure

We use the numerical method described in ref.4 to solve the governing equations presented in Section 2.1 and 2.2. This is an efficient two-point finite-difference method developed by Keller and Cebeci[4] and extensively used by Cebeci for two-dimensional and three-dimensional flows (see, for example, ref. 2). A detailed description is presented in ref. 2 and is not repeated here.

One of the advantages of the present numerical method is that nonuniform net spacings can be used in the x-direction as well as across the boundary layer. In the latter case, the nonuniform grid is a geometric progression with the property that the ratio of lengths of any two adjacent intervals is a constant; that is, $\Delta\eta_j = K\Delta\eta_{j-1}$. The distance to the j-th line is given by the following formula:

$$\Delta\eta_j = \Delta\eta_1 (K^j - 1)/(K - 1) \quad K > 1 \tag{2.33}$$

There are two parameters in (2.33): $\Delta\eta_1$, the length of the first step, and K, the ratio of two successive steps. The total number of points J can be calculated from the following formula:

$$J = \frac{\ln[1 + (K - 1)(\eta_\infty/\Delta\eta_1)]}{\ln K} + 1 \tag{2.34}$$

In the computer program which embodies the present solution method, $\Delta\eta_1$ and K are specified. For moderate Reynolds numbers, say R_x up to 10^7, typical values of $\Delta\eta_1$ and K are 0.01 and 1.14, respectively. In general, approximately 50 grid nodes across the boundary layer are sufficient to represent laminar and turbulent boundary layers. On the other hand, at higher Reynolds

numbers it is desirable and necessary to choose $\Delta\eta_1$ equal to 0.001 and K to 1.26, respectively.

In the present method, the flow is laminar at the stagnation point and can become turbulent at any specified station greater than second x-station (NX > 2). The present boundary-layer program does not compute the transition location and requires it to be input.

2.6 Boundary-Layer Parameters

The output of the computer program includes profiles of stream function, velocity and shear stress, i.e., f, f' and f" as a function of the similarity variable η and the physical distance y at calculation station x. Profiles for the total enthalpy E distribution and its derivative E' are also presented. The calculated boundary-layer parameters such as the local skin-friction coefficient c_f, the total drag, the various boundary-layer thicknesses and shape factors are summarized at the end of the output data. Expressed in either physical or transformed coordinates, these parameters are:

The local skin-friction coefficient:

$$c_f = \frac{2\tau_w}{\rho_e u_e^2} = \frac{2C_w}{R_{\tilde{x}}^{1/2}} \left(\frac{r_o}{L}\right) f''_w \tag{2.35}$$

The drag coefficient based on total frictional resistance D is:

$$C_F = \frac{2D}{\rho_\infty u_\infty^2 L^2} = \frac{2\pi}{L^2} \int_0^{x_t} c_f r_o \left(\frac{\rho_e}{\rho_\infty}\right)\left(\frac{u_e}{u_\infty}\right)^2 dx \tag{2.36}$$

Here L is any convenient reference length defined by the user and x is the axial distance from the nose of the body. The subscript t refers to the aft end of the body. To calculate the total drag of the body, use is made of Young's[5] formula, which can be written for compressible flow with average values in the wake as

$$C_D = \frac{2(\theta_A)_t}{L^2} \left(\frac{T_e}{T_\infty}\right)_t^{2.5} \left(\frac{u_e}{u_\infty}\right)_t^{(h_t+5+0.4M_\infty^2)/2} \tag{2.37}$$

Here θ_A is the momentum area defined by

$$\theta_A = 2\pi \int_0^\infty r \left(\frac{\rho}{\rho_e}\right)\left(\frac{u}{u_e}\right)\left(1 - \frac{u}{u_e}\right)dy = \frac{\bar{x}L}{R_{\bar{x}}^{1/2}} \int_0^\infty f'(1 - f')d\eta \tag{2.38}$$

and h is the shape factor based on the ratio of the displacement area δ_A^* to the momentum area θ_A; δ_A^* being defined by

$$\delta_A^* = 2\pi \int_0^\infty r \left(1 - \frac{\rho u}{\rho_e u_e}\right)dy = \frac{\bar{x}L}{R_{\bar{x}}^{1/2}} \int_0^\infty \left(\frac{\rho_e}{\rho} - f'\right)d\eta \tag{2.39}$$

Sometimes it is useful to examine integral thicknesses based on the profiles alone; that is, thin two-dimensional equivalents:

$$\delta_2^* = \int_0^\infty \left(1 - \frac{\rho u}{\rho_e u_e}\right)dy = \frac{\bar{x}}{R_{\bar{x}}^{1/2}} \left(\frac{L}{r_o}\right) \int_0^\infty \frac{(\rho_e/\rho - f')}{(1 + t)}\, dy \tag{2.40}$$

$$\theta_2 = \int_0^\infty \frac{\rho u}{\rho_e u_e} \left(1 - \frac{u}{u_e}\right)dy = \frac{\bar{x}}{R_{\bar{x}}^{1/2}} \left(\frac{L}{r_o}\right) \int_0^\infty \frac{f'(1 - f')}{(1 + t)}\, d\eta \tag{2.41}$$

$$H_2 = \frac{\delta_2^*}{\theta_2} \tag{2.42}$$

The height of the displacement surface, δ_3^* for axisymmetric flows with transverse curvature term included is defined by:

$$2\delta_3^* r_o + (\delta_3^*)^2 \cos\phi = 2 \int_0^\infty r \left(1 - \frac{\rho u}{\rho_e u_e}\right)dy = \frac{2\bar{x}L}{R_{\bar{x}}} \int_0^\infty \left(\frac{\rho}{\rho_e} - f'\right)d\eta = \frac{2\delta_A^*}{\pi} \tag{2.43}$$

or

$$\delta_3^* = \frac{r_o}{\cos\phi}\left[-1 + \left(1 + \frac{\delta_A^* \cos\phi}{\pi\, r_o^2}\right)^{1/2}\right] \tag{2.44}$$

Note that for $r_o >> \delta_3^*$ the above expression gives $\delta_3^* \to \delta_2^*$ as expected.

The boundary-layer thickness δ is obtained by interpolation for y where $u/u_e = 0.995$.

3.0 DESCRIPTION OF THE BOUNDARY-LAYER COMPUTER PROGRAM

3.1 Input

Given an axisymmetric body at zero incidence and the associated inviscid velocity distribution on the surface of the body, this program calculates the development of laminar and turbulent boundary layers with air or water as working medium. Surface boundary conditions allow for arbitrary wall mass transfer, wall temperature or heat transfer rate.

For air the external inviscid flow is treated as compressible isentropic flow. The external temperature and pressure distributions are calculated from the following formulas:

$$\frac{T_e}{T_\infty} = 1 - \frac{\gamma - 1}{2} M_\infty^2 \left[\left(\frac{u_e}{u_\infty} \right)^2 - 1 \right] \tag{3.1}$$

$$\frac{\rho_e}{\rho_\infty} = 1 - \frac{\gamma - 1}{2} M_\infty^2 \left[\left(\frac{u_e}{u_\infty} \right)^2 - 1 \right]^{\gamma/\gamma-1} \tag{3.2}$$

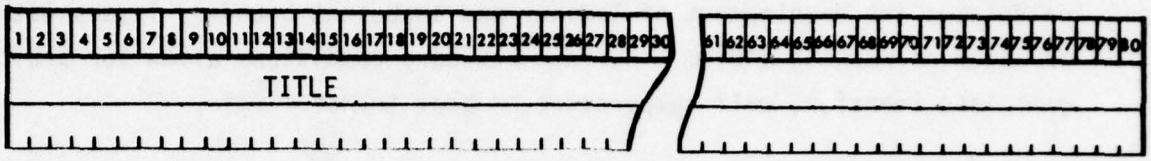
Here γ is the ratio of the specific heats at constant pressure and volume; its value is set equal to 1.4. The total enthalpy at the boundary-layer edge is calculated from

$$H_e = c_p T_e + \frac{u_e^2}{2} \tag{3.3}$$

and density is calculated from the perfect gas formula (2.7). The kinematic viscosity μ_e is calculated from (2.6).

For flows with water, either pure water or sea water, the fluid is assumed to be incompressible. That is, there is no Mach number effect but all fluid properties are allowed to be functions of temperature. In addition, the specific heat at constant pressure is assumed constant and equal to the average of the wall and freestream values. This is a reasonable assumption for the temperature levels and differences occurring in practice. As a result, the calculation of temperature from the total enthalpy is greatly simplified. Fluid properties for water are calculated by (2.8) to (2.17).

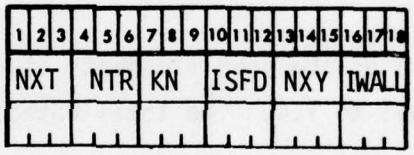
Essentially the input to the computer program consists of five types of cards. Card 1, shown below, contains the title of the flow problem under consideration.



Load Sheet for Card 1

The input is punched as 80-column alphanumeric field.

Card 2 requires the following information to be specified. The input is in 6I3 format.



Load Sheet for Card 2

NXT — total number of x-stations to be calculated NXT≥3

NTR — station number at which turbulent flow calculations start. NTR≥3 must be observed.

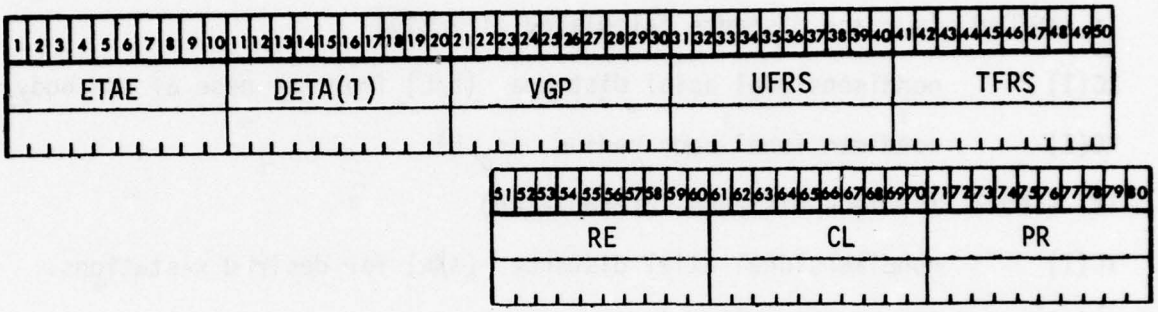
KN — this flag controls the type of fluid to be used in calculations
= 1 Air
= 2 Pure Water
= 3 Sea Water

ISFD — this flag controls the surface distance calculations. Usually we input pairs of the body coordinates at the x-stations where the boundary layer is to be calculated. But sometimes it is advantageous to use a different set of body coordinate data or input surface distance directly.
= 0 surface distance calculated directly at x-stations.
= 1 surface distance calculated from the separate body coordinate input and interpolated to desired x-stations.
= 2 surface distance input at x-stations.

NXY — number of body coordinate pairs for separate surface distance calculations. Used only if ISFD=1.

IWALL — flag that controls the wall boundary conditions for the energy equation.
= 1 wall temperature specified, °R.
= 2 wall heat transfer specified, Btu/hr/ft^2

Card 3 contains the following information to be specified. The input is in 8F10.0 format.



Load Sheet for Card 3

ETAE — transformed boundary-layer thickness, η_∞. This is for the first station. A value of 6 is usually sufficient. For NX>1, the boundary-layer thickness is computed internally.

DETA(1) — initial $\Delta\eta$-spacing at the wall, $\Delta\eta_1$.

VGP — variable grid parameter, K.

UFRS — freestream velocity u_∞, (ft/sec)

TFRS — freestream static temperature (°R)

RE — unit Reynolds number based on freestream conditions, $Re_\infty/ft = u_\infty/\nu_\infty$.

CL — reference length L. Converts nondimensional body coordinates into dimensional form, expressed in feet.

PR — Prandtl number for air. Can be ignored for calculations with water.

The fourth and the following cards contain the information for surface distance calculation, the external velocity, surface temperature or heat transfer, and mass transfer at the wall. There will be NXT cards of this type. A sample load sheet for this case is shown below. The format is 5F10.0.

1 2 3 4 5 6 7 8 9 10	11 12 13 14 15 16 17 18 19 20	21 22 23 24 25 26 27 28 29 30	31 32 33 34 35 36 37 38 39 40	41 42 43 44 45 46 47 48 49 50
XC(I)	RC(I)	UE(I)	HTP(I)	BV(I)

Load Sheet for Card 5

If ISFD=0 (surface distance calculated directly)

XC(I) nondimensional axial distance (X/L) from the nose of the body.

RC(I) nondimensional body radius (r_o/L)

If ISFD=1 (surface distance interpolated)

XC(I) nondimensional axial distance (X/L) for desired x-stations.

RC(I) can be left blank.

If ISFD=2 (surface distance input)

XC(I) nondimensional surface distance (x/L) input.

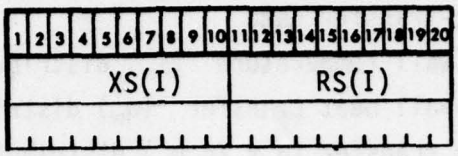
RC(I) nondimensional body radius (r_o/L) input at stations corresponding to (x/L) input.

UE(I) nomdimensional velocity distribution (u_e/u_∞) input at x-stations.

HTP(I) dimensional wall temperature or heat transfer.
If IWALL=1 the wall temperature (T_w) is input, °R.
If IWALL=2 the heat transfer rate at the wall (q_w) is input; Btu/hr/ft^2.

BV(I) nondimensional mass-transfer ratio at the wall, $\rho_w v_w/\rho_e u_e$. For no mass-transfer, leave blank.

If ISFD=1 (surface distance interpolated) additional data is needed for the separate body definition cards. These are in the form of axial distance ($\bar{X}$/L) and body radius (r_o/L) pairs. There are NXY cards of this type. A sample load sheet for this case is shown below. The format is 2F10.0.



Load Sheet for Body Coordinates

XS(I) nondimensional axial distance (X/L) from body nose.

RS(I) nondimensional body radius (r_o/L).

3.2 Output

The output of the computer program includes printout of the data used in boundary-layer calculations as well as tables of profile data at all x-stations. At the end of the printout is a summary of the calculated boundary-layer parameter. Boundary-layer calculation data is presented under the headings of CASE DATA and STATION DATA:

CASE DATA: Data is printed out in two groups. The first group contains the flags and control variables specified in the input. The second group pertains to the input and calculated freestream data.

UFRS freestream velocity (u_∞), ft/sec.

TFRS freestream static temperature (T_∞), °R.

PFRS freestream static pressure (P_∞), lb/ft^2.

RHOFRS freestream density (ρ_∞), slugs/ft^3.

PRFRS Prandtl number for air.

RMUI freestream dynamic viscosity (μ_∞), lb-sec/ft^2

RCI unit Reynolds number based on freestream (u_∞/ν_∞), ft^{-1}

Note that for air there is additional printout for the freestream Mach number (M_∞) and the freestream total temperature (T_T), °R.

STATION DATA: refers to a table with the following columns.

NX station number of the x-station

X calculated or input surface distance x, ft

RC — input or interpolated nondimensional body radius (r_o/L)

UE — inviscid velocity at an x-station, ft/sec.

HTP — input heat-transfer data
IWALL=1, wall temperature (T_w) distribution, °R.
=2, wall heat transfer (q_w) distribution, Btu/hr/ft^2

BV — input mass transfer ($\rho_w v_w/\rho_e u_e$) distribution

PZ — calculated pressure gradient parameter ($m_2 = \bar{x}/u_e \; du_e/d\bar{x}$)

The profile data is presented in tables identified by a printout line containing the station number NX, the surface distance x, and the surface distance Mangler variable XB($\bar{x}$). The next few lines before the table proper refer to the iterations during calculations. The columns in the table contain the following:

J — point number: profiles are plotted from the wall outward. Not all points are printed.

ETA — nondimensional boundary-layer variable η.

U — nondimensional velocity in the boundary layer, $f' = u/u_e$.

V — derivative of U with respect to η, f".

W — nondimensional total enthalpy ratio, $E = H/H_e$.

T — derivative of W with respect to η, E'.

TEMP — static temperature in the boundary layer, °R.

Y — normal distance from the surface y, ft

OUTPUT SUMMARY: This table at the very end of the output contains some input data and the calculated boundary-layer parameters in 9 columns with two rows per NX-station.

First row

NX — the x-station number

X — surface distance (x), ft

UE — inviscid velocity (u_e), ft/sec

DEL — boundary-layer thickness δ, y-value where $u/u_e = 0.995$.

MOMA — momentum area θ_A, ft^2

MOM2 — two-dimensional momentum thickness θ_2, ft

CF — local skin-friction coefficient, $c_f = 2\tau_w/\rho_e u_e^2$

CD total drag coefficient of the body C_D, calculated by Young's formula. Reference area is the input reference length (L) squared.

TW wall temperature (T_w), °R.

Second Row

X/C the axial nondimensional distance from the nose of the body. If surface distance is input (ISFD=2) the input nondimensional x is printed out.

RX local Reynolds number $Re = u_e x/\nu_e$

DISPA displacement area δ_A^*, ft^2

HA shape factor used in total drag formula $H_A = \delta_A^*/\theta_A$

H2 two-dimensional shape factor $H_2 = \delta_2^*/\theta_2$

CT the average integrated skin-friction coefficient of the body, C_F

DISPLT displacement thickness for axisymmetric body δ_3^*, ft

QW heat transfer rate on the body surface $q_w = -k_w \partial T/\partial y$, $Btu/hr/ft^2$

3.3 Sample Calculations

The present computer program can be used to determine the properties of axisymmetric laminar and turbulent boundary layers in air or water over smooth surfaces with wall mass transfer, arbitrary wall temperature or heat transfer. Flows in air are treated as compressible and flows in water as incompressible, but with allowance for temperature-dependent fluid properties. In order to demonstrate its capability and input requirements, we present these sample calculations for the same body representing flows in different fluids and at different wall boundary conditions.

The body called 5A has a fineness ratio of 6 2/3 and its profile is formed by a modified NACA 4-digit thickness distribution with maximum thickness at 45 percent. Its nose radius and trailing-edge angle are standard. The body length is 20 ft and all runs were made at a length Reynolds number of 40×10^6. This combined with a freestream temperature of 520°R corresponds to a freestream velocity of 570 fps in air and 35 fps in water. Transition is fixed at about 21 percent of chord (station 15) for all cases. The external inviscid flow was calculated by the Douglas Neumann program. It should be noted that no compressibility corrections were applied to the calculation in air although the freestream Mach number was 0.5.

The sample case for flow in air was computed with adiabatic wall boundary conditions; that is, $q_w = 0$, and suction was applied to the rear portion of the body from approximately 56 percent chord-point onward. The input data, typical turbulent boundary-layer profiles with suction at 81-percent chord (station 39), and the summary of calculated data are shown below. It should be noted that in this, as well as in two other cases, boundary layers separate at the last calculation station. This is expected since the inviscid flow at the aft end of the body approaches a stagnation point: If the pressure changes due to viscous interaction are not accounted for, continued boundary-layer calculations will result in inevitable separation.

BODY 5A IN AIR

BEST AVAILABLE COPY

** CASE DATA

NXT	= 46	NTR	= 15	KN	= 1			
IWALL	= 2	ISED	= 0	NXY	= 46			
ETAE	= 0.600000E+01	DETA1	= 0.100000E-02	VGP	= 0.114000E+01	CL	=	0.200000E+02
UFRS	= 0.570000E+03	TFRS	= 0.540000E+03	PFRS	= 0.125393E+04			
RHOFRS	= 0.135320E-02	PRFRS	= 0.720000E+00	RMUI	= 0.385662E-06	RCI	=	0.200000E+07

** FOR AIR

MFRS = 0.500447E+00 TTOTL = 0.567048E+03

** STATION DATA

NX	X	RC	UE		HTP	BV	P2
1	0.0	0.0	0.0	0.0		0.0	0.333333E+00
2	0.700318E-01	0.349200E-02	0.973075E+02	0.0		0.0	0.479140E+00
3	0.181736E+00	0.889500E-02	0.235714E+03	0.0		0.0	0.327130E+00
4	0.273307E+00	0.130170E-01	0.326641E+03	0.0		0.0	0.266799E+00
5	0.400303E+00	0.181760E-01	0.416488E+03	0.0		0.0	0.209588E+00
6	0.605241E+00	0.252220E-01	0.500068E+03	0.0		0.0	0.146102E+00
7	0.876230E+00	0.326590E-01	0.551984E+03	0.0		0.0	0.917818E-01
8	0.120895E+01	0.398110E-01	0.579571E+03	0.0		0.0	0.561251E-01
9	0.165969E+01	0.472930E-01	0.595711E+03	0.0		0.0	0.322510E-01
10	0.217736E+01	0.538310E-01	0.602856E+03	0.0		0.0	0.156482E-01
11	0.268754E+01	0.588070E-01	0.605117E+03	0.0		0.0	0.531318E-02
12	0.319373E+01	0.626960E-01	0.605313E+03	0.0		0.0	-0.195386E-02
13	0.369758E+01	0.657670E-01	0.604400E+03	0.0		0.0	-0.801632E-02
14	0.419999E+01	0.681920E-01	0.602857E+03	0.0		0.0	-0.133218E-01
15	0.470148E+01	0.700960E-01	0.600941E+03	0.0		0.0	-0.130985E-01
16	0.520239E+01	0.715730E-01	0.598809E+03	0.0		0.0	-0.223981E-01
17	0.570291E+01	0.726970E-01	0.596571E+03	0.0		0.0	-0.261741E-01
18	0.620319E+01	0.735310E-01	0.594309E+03	0.0		0.0	-0.293437E-01
19	0.670335E+01	0.741260E-01	0.592085E+03	0.0		0.0	-0.317462E-01
20	0.720341E+01	0.745290E-01	0.589959E+03	0.0		0.0	-0.330630E-01
21	0.770344E+01	0.747320E-01	0.587996E+03	0.0		0.0	-0.328531E-01
22	0.820345E+01	0.749210E-01	0.586273E+03	0.0		0.0	-0.303190E-01
23	0.870345E+01	0.749830E-01	0.584882E+03	0.0		0.0	-0.232291E-01
24	0.920345E+01	0.750000E-01	0.584068E+03	0.0		0.0	-0.650376E-02
25	0.970345E+01	0.749990E-01	0.584299E+03	0.0		0.0	0.182632E-01
26	0.102034E+02	0.749750E-01	0.585535E+03	0.0		0.0	0.391307E-01
27	0.107035E+02	0.748900E-01	0.587251E+03	0.0		0.0	0.510086E-01
28	0.112035E+02	0.746980E-01	0.589147E+03	0.0		0.0	0.572936E-01
29	0.117035E+02	0.743580E-01	0.591071E+03	0.0		-0.500000E-03	0.597217E-01

BEST AVAILABLE COPY

30	0.122036E+02	0.738280E-01	0.592898E+03	0.0	-0.500000E-03	0.580368E-01
31	0.127039E+02	0.730650E-01	0.594506E+03	0.0	-0.500000E-03	0.522938E-01
32	0.132043E+02	0.720280E-01	0.595785E+03	0.0	-0.500000E-03	0.408486E-01
33	0.137051E+02	0.706740E-01	0.596610E+03	0.0	-0.600000E-03	0.230358E-01
34	0.142063E+02	0.689610E-01	0.596855E+03	0.0	-0.800000E-03	-0.520033E-02
35	0.147081E+02	0.668460E-01	0.596381E+03	0.0	-0.100000E-02	-0.449661E-01
36	0.152107E+02	0.642870E-01	0.595037E+03	0.0	-0.120000E-02	-0.103577E+00
37	0.157144E+02	0.612420E-01	0.592656E+03	0.0	-0.140000E-02	-0.190348E+00
38	0.162196E+02	0.576680E-01	0.589039E+03	0.0	-0.150000E-02	-0.319889E+00
39	0.167264E+02	0.535240E-01	0.583970E+03	0.0	-0.150000E-02	-0.520696E+00
40	0.172355E+02	0.487670E-01	0.577173E+03	0.0	-0.150000E-02	-0.848511E+00
41	0.177471E+02	0.433550E-01	0.568308E+03	0.0	-0.150000E-02	-0.142300E+01
42	0.182619E+02	0.372450E-01	0.556905E+03	0.0	-0.150000E-02	-0.254138E+01
43	0.187804E+02	0.303950E-01	0.542238E+03	0.0	-0.150000E-02	-0.509478E+01
44	0.193032E+02	0.227630E-01	0.523003E+03	0.0	-0.150000E-02	-0.128093E+02
45	0.198311E+02	0.143060E-01	0.495911E+03	0.0	-0.150000E-02	-0.531138E+02
46	0.203649E+02	0.498300E-02	0.450411E+03	0.0	-0.150000E-02	-0.723735E+03

NX= 39 X= 0.16726E+02 XB= 0.74619E-01
V(1,2)= 0.112493E+02 DELV(1)= 0.816469E+00
V(1,2)= 0.120657E+02 DELV(1)= 0.195019E-01

J	ETA	U	V	W	T	TEMP	Y
1	0.0	0.0	0.120852E+02	0.999542E+00	0.0	0.566788E+03	0.0
5	0.00492	0.578812E-01	0.114400E+02	0.999566E+00	0.932886E-02	0.566706E+03	0.185016E-04
9	0.01323	0.148051E+00	0.101950E+02	0.999692E+00	0.198989E-01	0.566250E+03	0.497349E-04
13	0.02727	0.270171E+00	0.708275E+01	0.999988E+00	0.189238E-01	0.564969E+03	0.102401E-03
17	0.05098	0.387362E+00	0.332820E+01	0.100025E+01	0.498777E-02	0.562930E+03	0.191063E-03
21	0.09103	0.472933E+00	0.136611E+01	0.100032E+01	0.112317E-03	0.560878E+03	0.340225E-03
25	0.15866	0.532976E+00	0.536623E+00	0.100031E+01	-0.227843E-03	0.559157E+03	0.591265E-03
29	0.27289	0.578695E+00	0.230488E+00	0.100028E+01	-0.195807E-03	0.557700E+03	0.101396E-02
33	0.46582	0.617469E+00	0.147774E+00	0.100025E+01	-0.147906E-03	0.556365E+03	0.172579E-02
37	0.79168	0.653335E+00	0.845789E-01	0.100021E+01	-0.109885E-03	0.555047E+03	0.292419E-02
41	1.34203	0.687962E+00	0.471059E-01	0.100016E+01	-0.551112E-04	0.553704E+03	0.494048E-02
45	2.27156	0.721342E+00	0.280869E-01	0.100013E+01	-0.317219E-04	0.552347E+03	0.832915E-02
49	3.84149	0.754812E+00	0.166600E-01	0.100009E+01	-0.166859E-04	0.550924E+03	0.140145E-01
53	6.49306	0.787751E+00	0.969831E-02	0.100006E+01	-0.754512E-05	0.549465E+03	0.235262E-01
57	10.97145	0.822259E+00	0.692023E-02	0.100004E+01	-0.373960E-05	0.547874E+03	0.393652E-01
61	18.53526	0.872590E+00	0.624102E-02	0.100002E+01	-0.189027E-05	0.545441E+03	0.655279E-01
65	31.31024	0.938282E+00	0.396929E-02	0.100000E+01	-0.499492E-06	0.542056E+03	0.108183E+00
69	52.88673	0.986401E+00	0.104273E-02	0.100000E+01	0.729597E-07	0.539312E+03	0.176562E+00
72	78.35751	0.100000E+01	0.146236E-03	0.100000E+01	-0.685728E-07	0.538657E+03	0.252586E+00

OUTPUT SUMMARY

NX	X X/C	UE RX	DEL DISPA	MOMA HA	MOM2 H2	CF CFT	CD DISPLT	TW QW
1	0.0 0.0	0.0 0.0	0.33165E-03 0.0	0.0 0.0	0.10798E-03 0.22971E+01	0.0 0.0	0.0 0.24804E-03	0.56705E+03 0.0
2	0.70032E-01 0.25900E-03	0.97303E+02 0.25965E+05	0.10668E-02 0.12060E-03	0.53409E-04 0.22580E+01	0.12167E-03 0.22583E+01	0.15300E-01 0.35667E-11	0.49211E-09 0.27462E-03	0.56693E+03 0.0
3	0.18174E+00 0.16740E-02	0.23571E+03 0.16130E+06	0.10103E-02 0.30258E-03	0.12980E-03 0.23311E+01	0.11607E-03 0.23315E+01	0.62123E-02 0.13932E-09	0.28230E-07 0.27055E-03	0.56647E+03 0.0
4	0.27331E+00 0.36670E-02	0.32664E+03 0.33174E+06	0.10962E-02 0.50195E-03	0.21106E-03 0.23783E+01	0.12895E-03 0.23788E+01	0.39991E-02 0.59373E-09	0.14698E-06 0.30686E-03	0.56625E+03 0.0
5	0.40030E+00 0.73690E-02	0.41649E+03 0.60386E+06	0.12535E-02 0.81511E-03	0.33667E-03 0.24211E+01	0.14730E-03 0.24217E+01	0.27344E-02 0.19510E-08	0.55665E-06 0.35678E-03	0.56568E+03 0.0
6	0.60524E+00 0.14500E-01	0.50007E+03 0.10833E+07	0.15540E-02 0.14503E-02	0.57895E-03 0.25051E+01	0.18252E-03 0.25058E+01	0.17680E-02 0.56575E-08	0.18228E-05 0.45717E-03	0.56530E+03 0.0
7	0.87623E+00 0.26135E-01	0.55198E+03 0.17062E+07	0.19334E-02 0.24395E-02	0.94803E-03 0.25732E+01	0.23080E-03 0.25740E+01	0.12175E-02 0.12142E-07	0.42301E-05 0.59393E-03	0.56494E+03 0.0
8	0.12089E+01 0.41155E-01	0.57957E+03 0.24513E+07	0.24235E-02 0.38153E-02	0.14449E-02 0.26405E+01	0.28853E-03 0.26414E+01	0.87590E-03 0.20810E-07	0.76663E-05 0.76197E-03	0.56488E+03 0.0
9	0.16597E+01 0.62414E-01	0.59571E+03 0.34414E+07	0.29886E-02 0.57503E-02	0.21416E-02 0.26850E+01	0.35997E-03 0.26860E+01	0.65731E-03 0.32408E-07	0.12540E-04 0.96680E-03	0.56471E+03 0.0
10	0.21774E+01 0.87458E-01	0.60286E+03 0.45285E+07	0.35734E-02 0.80433E-02	0.29498E-02 0.27267E+01	0.43555E-03 0.27278E+01	0.51203E-03 0.44984E-07	0.18044E-04 0.11885E-02	0.56476E+03 0.0
11	0.26875E+01 0.11248E+00	0.60512E+03 0.56435E+07	0.41411E-02 0.10281E-01	0.37383E-02 0.27503E+01	0.50521E-03 0.27515E+01	0.42826E-03 0.56442E-07	0.23191E-04 0.13906E-02	0.56466E+03 0.0
12	0.31937E+01 0.13749E+00	0.60531E+03 0.67082E+07	0.47051E-02 0.12489E-01	0.45043E-02 0.27727E+01	0.57093E-03 0.27740E+01	0.36742E-03 0.66950E-07	0.27995E-04 0.15842E-02	0.56475E+03 0.0
13	0.36976E+01 0.16249E+00	0.60440E+03 0.77571E+07	0.52319E-02 0.14627E-01	0.52473E-02 0.27876E+01	0.63399E-03 0.27890E+01	0.32498E-03 0.76617E-07	0.32450E-04 0.17681E-02	0.56469E+03 0.0
14	0.42000E+01 0.18749E+00	0.60286E+03 0.87930E+07	0.57409E-02 0.16737E-01	0.59687E-02 0.28042E+01	0.69544E-03 0.28057E+01	0.28950E-03 0.85535E-07	0.36589E-04 0.19510E-02	0.56477E+03 0.0
15	0.47015E+01 0.21250E+00	0.60094E+03 0.98177E+07	0.86236E-02 0.14567E-01	0.81506E-02 0.17873E+01	0.92367E-03 0.17880E+01	0.15885E-02 0.11377E-06	0.48082E-04 0.16519E-02	0.56527E+03 0.0
16	0.52024E+01 0.23750E+00	0.59881E+03 0.10833E+08	0.15304E-01 0.20178E-01	0.13059E-01 0.15451E+01	0.14476E-02 0.15459E+01	0.26972E-02 0.17903E-06	0.75735E-04 0.22414E-02	0.56643E+03 0.0
17	0.57029E+01 0.26250E+00	0.59557E+03 0.11839E+08	0.22917E-01 0.29006E-01	0.19473E-01 0.14896E+01	0.21223E-02 0.14906E+01	0.27688E-02 0.26311E-06	0.11154E-03 0.31715E-02	0.56644E+03 0.0

BEST AVAILABLE COPY

BEST AVAILABLE COPY

18	0.62032E+01	0.59431E+03	0.30328E-01	0.26017E-01	0.27994E-02	0.27227E-02	0.14727E-03	0.56644E+03
	0.28750E+00	0.12833E+08	0.38197E-01	0.14682E+01	0.14693E+01	0.34815E-06	0.41270E-02	0.0
19	0.67034E+01	0.59208E+03	0.37673E-01	0.32557E-01	0.34702E-02	0.25961E-02	0.18222E-03	0.56655E+03
	0.31250E+00	0.13831E+08	0.47350E-01	0.14543E+01	0.14557E+01	0.43079E-06	0.50743E-02	0.0
20	0.72034E+01	0.58996E+03	0.45318E-01	0.39007E-01	0.41295E-02	0.25541E-02	0.21596E-03	0.56642E+03
	0.33750E+00	0.14819E+08	0.56293E-01	0.14432E+01	0.14447E+01	0.51084E-06	0.59982E-02	0.0
21	0.77034E+01	0.58800E+03	0.52853E-01	0.45336E-01	0.47770E-02	0.24551E-02	0.24852E-03	0.56660E+03
	0.36250E+00	0.15805E+08	0.65118E-01	0.14363E+01	0.14381E+01	0.58358E-06	0.69125E-02	0.0
22	0.82034E+01	0.58627E+03	0.59560E-01	0.51497E-01	0.54089E-02	0.24269E-02	0.27983E-03	0.56644E+03
	0.38750E+00	0.16791E+08	0.73609E-01	0.14294E+01	0.14313E+01	0.66413E-06	0.77982E-02	0.0
23	0.87034E+01	0.58468E+03	0.66904E-01	0.57438E-01	0.60203E-02	0.23634E-02	0.30991E-03	0.56666E+03
	0.41250E+00	0.17780E+08	0.81830E-01	0.14247E+01	0.14268E+01	0.73810E-06	0.86598E-02	0.0
24	0.92034E+01	0.58407E+03	0.72290E-01	0.63030E-01	0.65972E-02	0.23519E-02	0.33867E-03	0.56644E+03
	0.43750E+00	0.18780E+08	0.89505E-01	0.14200E+01	0.14222E+01	0.81071E-06	0.94671E-02	0.0
25	0.97034E+01	0.58430E+03	0.77361E-01	0.68133E-01	0.71236E-02	0.23168E-02	0.36650E-03	0.56668E+03
	0.46250E+00	0.19806E+08	0.96519E-01	0.14166E+01	0.14190E+01	0.88247E-06	0.10207E-01	0.0
26	0.10203E+02	0.58594E+03	0.83889E-01	0.73142E-01	0.76404E-02	0.23128E-02	0.39588E-03	0.56641E+03
	0.48750E+00	0.20863E+08	0.10317E+00	0.14105E+01	0.14130E+01	0.95377E-06	0.10910E-01	0.0
27	0.10703E+02	0.58725E+03	0.90390E-01	0.77920E-01	0.81389E-02	0.22922E-02	0.42536E-03	0.56667E+03
	0.51250E+00	0.21937E+08	0.10965E+00	0.14072E+01	0.14098E+01	0.10250E-05	0.11606E-01	0.0
28	0.11203E+02	0.58915E+03	0.97833E-01	0.82515E-01	0.86303E-02	0.22741E-02	0.45470E-03	0.56645E+03
	0.53750E+00	0.23023E+08	0.11582E+00	0.14036E+01	0.14064E+01	0.10958E-05	0.12237E-01	0.0
29	0.11704E+02	0.59107E+03	0.10448E+00	0.86158E-01	0.90413E-02	0.25562E-02	0.47924E-03	0.56660E+03
	0.56250E+00	0.24114E+08	0.12001E+00	0.13929E+01	0.13958E+01	0.11709E-05	0.12788E-01	0.0
30	0.12204E+02	0.59290E+03	0.11035E+00	0.89047E-01	0.93994E-02	0.26230E-02	0.49970E-03	0.56648E+03
	0.58750E+00	0.25203E+08	0.12316E+00	0.13830E+01	0.13860E+01	0.12513E-05	0.13216E-01	0.0
31	0.12704E+02	0.59451E+03	0.11617E+00	0.92036E-01	0.98027E-02	0.26051E-02	0.52052E-03	0.56668E+03
	0.61250E+00	0.26299E+08	0.12632E+00	0.13780E+01	0.13810E+01	0.13323E-05	0.13747E-01	0.0
32	0.13204E+02	0.59578E+03	0.12345E+00	0.95105E-01	0.10259E-01	0.26102E-02	0.54121E-03	0.56652E+03
	0.63750E+00	0.27382E+08	0.13066E+00	0.13738E+01	0.13771E+01	0.14124E-05	0.14363E-01	0.0
33	0.13705E+02	0.59661E+03	0.13146E+00	0.98138E-01	0.10769E-01	0.26488E-02	0.56067E-03	0.56670E+03
	0.66250E+00	0.28453E+08	0.13443E+00	0.13698E+01	0.13733E+01	0.14920E-05	0.15056E-01	0.0
34	0.14206E+02	0.59685E+03	0.13973E+00	0.10092E+00	0.11324E-01	0.27887E-02	0.57716E-03	0.56651E+03
	0.68750E+00	0.29503E+08	0.13761E+00	0.13636E+01	0.13672E+01	0.15727E-05	0.15789E-01	0.0
35	0.14708E+02	0.59633E+03	0.14864E+00	0.10344E+00	0.11943E-01	0.29350E-02	0.59015E-03	0.56668E+03
	0.71250E+00	0.30525E+08	0.14036E+00	0.13569E+01	0.13607E+01	0.16553E-05	0.16606E-01	0.0
36	0.15211E+02	0.59504E+03	0.15863E+00	0.10584E+00	0.12663E-01	0.30817E-02	0.59979E-03	0.56659E+03
	0.73751E+00	0.31511E+08	0.14285E+00	0.13497E+01	0.13538E+01	0.17389E-05	0.17563E-01	0.0

37	0.15714E+02	0.59266E+03	0.17024E+00	0.10828E+00	0.13540E-01	0.32433E-02	0.60641E-03	0.56672E+03
	0.76251E+00	0.32449E+08	0.14537E+00	0.13426E+01	0.13470E+01	0.18225E-05	0.18746E-01	0.0
38	0.16220E+02	0.58004E+03	0.18419E+00	0.11106E+00	0.14664E-01	0.33085E-02	0.61097E-03	0.56668E+03
	0.78751E+00	0.33526E+08	0.14843E+00	0.13366E+01	0.13415E+01	0.19039E-05	0.20306E-01	0.0
39	0.16726E+02	0.58397E+03	0.20350E+00	0.11460E+00	0.16176E-01	0.32761E-02	0.61481E-03	0.56682E+03
	0.81251E+00	0.34125E+08	0.15269E+00	0.13324E+01	0.13381E+01	0.19795E-05	0.22469E-01	0.0
40	0.17235E+02	0.57717E+03	0.22792E+00	0.11926E+00	0.18270E-01	0.32021E-02	0.61841E-03	0.56678E+03
	0.83752E+00	0.34828E+08	0.15861E+00	0.13299E+01	0.13368E+01	0.20468E-05	0.25552E-01	0.0
41	0.17747E+02	0.56831E+03	0.25943E+00	0.12547E+00	0.21257E-01	0.31159E-02	0.62192E-03	0.56685E+03
	0.86252E+00	0.35407E+08	0.16676E+00	0.13292E+01	0.13378E+01	0.21045E-05	0.30098E-01	0.0
42	0.18262E+02	0.55691E+03	0.30147E+00	0.13398E+00	0.25716E-01	0.29823E-02	0.62591E-03	0.56683E+03
	0.88752E+00	0.35825E+08	0.17833E+00	0.13311E+01	0.13426E+01	0.21519E-05	0.37199E-01	0.0
43	0.18780E+02	0.54224E+03	0.36002E+00	0.14629E+00	0.32813E-01	0.27786E-02	0.63188E-03	0.56692E+03
	0.91253E+00	0.36026E+08	0.19570E+00	0.13377E+01	0.13547E+01	0.21880E-05	0.49308E-01	0.0
44	0.19303E+02	0.52300E+03	0.44701E+00	0.16642E+00	0.45354E-01	0.24403E-02	0.64563E-03	0.56696E+03
	0.93753E+00	0.35910E+08	0.22560E+00	0.13556E+01	0.13842E+01	0.22125E-05	0.73233E-01	0.0
45	0.19831E+02	0.49991E+03	0.60865E+00	0.21572E+00	0.73600E-01	0.16962E-02	0.71125E-03	0.56710E+03
	0.96253E+00	0.35238E+08	0.30539E+00	0.14157E+01	0.14835E+01	0.22256E-05	0.13824E+00	0.0

BEST AVAILABLE COPY

The second sample case is for flow in pure water (KN=2) where the nose portion of the body under the laminar boundary layer was heated. A moderate heat flux amounting to 1 Btu/sec/ft^2 was specified over most of the area, with less near the nose where a strong favorable pressure gradient exists. The input and output data for this second sample case are shown below.

BODY 5A IN WATER, WALL HEAT TRANS. SPEC.

** CASE DATA

NXT	= 46	NTR	= 15	KN	= 2			
IWALL	= 2	ISFD	= 0	NXY	= 46			
ETAE	= 0.600000E+01	DETA1	= 0.100000E-02	VGP	= 0.114000E+01	CL	=	0.200000E+02
UFRS	= 0.350000E+02	TFRS	= 0.520000E+03	PFRS	= 0.125393E+04			
RHOFRS	= 0.193783E+01	PRFRS	= 0.801097E+01	RMUI	= 0.234155E-04	RCI	=	0.200000E+07

** STATION DATA

NX	X	RC	UE	HTP		BV	P2
1	0.0	0.0	0.0	0.900000E+03	0.0		0.333333E+00
2	0.700316E-01	0.349200E-02	0.597502E+01	0.180000E+04	0.0		0.479140E+00
3	0.181736E+00	0.689560E-02	0.144737E+02	0.270000E+04	0.0		0.327130E+00
4	0.273307E+00	0.130170E-01	0.200569E+02	0.360000E+04	0.0		0.266799E+00
5	0.400303E+00	0.181760E-01	0.255738E+02	0.360000E+04	0.0		0.209588E+00
6	0.605241E+00	0.252220E-01	0.307059E+02	0.360000E+04	0.0		0.146102E+00
7	0.876230E+00	0.326590E-01	0.338938E+02	0.360000E+04	0.0		0.917816E-01
8	0.120895E+01	0.398110E-01	0.355877E+02	0.360000E+04	0.0		0.561246E-01
9	0.165966E+01	0.472920E-01	0.365788E+02	0.360000E+04	0.0		0.322511E-01
10	0.217736E+01	0.538310E-01	0.370175E+02	0.360000E+04	0.0		0.156481E-01
11	0.263754E+01	0.588070E-01	0.371563E+02	0.360000E+04	0.0		0.531347E-02
12	0.319373E+01	0.626960E-01	0.371683E+02	0.360000E+04	0.0		-0.195345E-02
13	0.369758E+01	0.657670E-01	0.371123E+02	0.360000E+04	0.0		-0.801672E-02
14	0.419999E+01	0.681920E-01	0.370175E+02	0.360000E+04	0.0		-0.133215E-01
15	0.470146E+01	0.700960E-01	0.368999E+02	0.360000E+04	0.0		-0.180987E-01
16	0.520239E+01	0.715730E-01	0.367690E+02	0.0	0.0		-0.223988E-01
17	0.570291E+01	0.726970E-01	0.366316E+02	0.0	0.0		-0.261743E-01
18	0.620316E+01	0.735310E-01	0.364926E+02	0.0	0.0		-0.293441E-01
19	0.670335E+01	0.741260E-01	0.363561E+02	0.0	0.0		-0.317452E-01
20	0.720341E+01	0.745290E-01	0.362256E+02	0.0	0.0		-0.330622E-01
21	0.770344E+01	0.747820E-01	0.361052E+02	0.0	0.0		-0.328529E-01
22	0.820345E+01	0.749210E-01	0.359992E+02	0.0	0.0		-0.303174E-01
23	0.870345E+01	0.749830E-01	0.359138E+02	0.0	0.0		-0.232297E-01
24	0.920345E+01	0.750000E-01	0.358638E+02	0.0	0.0		-0.650577E-02
25	0.970345E+01	0.749990E-01	0.358779E+02	0.0	0.0		0.182705E-01
26	0.102034E+02	0.749750E-01	0.359539E+02	0.0	0.0		0.391323E-01
27	0.107035E+02	0.748900E-01	0.360593E+02	0.0	0.0		0.510035E-01
28	0.112035E+02	0.746980E-01	0.361757E+02	0.0	0.0		0.572916E-01
29	0.117035E+02	0.743580E-01	0.362939E+02	0.0	0.0		0.597221E-01
30	0.122036E+02	0.738280E-01	0.364060E+02	0.0	0.0		0.580343E-01
31	0.127036E+02	0.730650E-01	0.365048E+02	0.0	0.0		0.522920E-01
32	0.132043E+02	0.720280E-01	0.365833E+02	0.0	0.0		0.408520E-01
33	0.137051E+02	0.706740E-01	0.366340E+02	0.0	0.0		0.230363E-01
34	0.142063E+02	0.689610E-01	0.366490E+02	0.0	0.0		-0.519674E-02
35	0.147081E+02	0.668460E-01	0.366199E+02	0.0	0.0		-0.449742E-01

BEST AVAILABLE COPY

BEST AVAILABLE COPY

36	0.152107E+02	0.642870E-01	0.365374E+02	0.0	0.0	-0.103579E+00
37	0.157144E+02	0.612420E-01	0.363911E+02	0.0	0.0	-0.190353E+00
38	0.162196E+02	0.576680E-01	0.361691E+02	0.0	0.0	-0.319893E+00
39	0.167264E+02	0.535240E-01	0.358578E+02	0.0	0.0	-0.520694E+00
40	0.172355E+02	0.487670E-01	0.354404E+02	0.0	0.0	-0.848496E+00
41	0.177471E+02	0.433550E-01	0.348961E+02	0.0	0.0	-0.142302E+01
42	0.182619E+02	0.372450E-01	0.341959E+02	0.0	0.0	-0.254137E+01
43	0.187804E+02	0.303950E-01	0.332953E+02	0.0	0.0	-0.509481E+01
44	0.193032E+02	0.227630E-01	0.321142E+02	0.0	0.0	-0.128093E+02
45	0.198311E+02	0.143060E-01	0.304507E+02	0.0	0.0	-0.531136E+02
46	0.203649E+02	0.498300E-02	0.276568E+02	0.0	0.0	-0.723739E+03

OUTPUT SUMMARY

NX	X X/C	UE RX	DEL DISPA	MOMA HA	MOM2 H2	CF CFT	CD DISPLT	TW QW
1	0.0 0.0	0.0 0.0	0.80674E-03 0.0	0.0 0.0	0.93435E-04 0.22938E+01	0.0 0.0	0.0 0.21432E-03	0.52068E+03 0.90000E+03
2	0.70032E-01 0.25900E-03	0.59750E+01 0.49101E+05	0.88934E-03 0.98418E-04	0.44521E-04 0.22106E+01	0.10143E-03 0.22109E+01	0.13455E-01 0.27735E-11	0.43125E-09 0.22420E-03	0.52121E+03 0.18000E+04
3	0.18174E+00 0.16740E-02	0.14474E+02 0.30864E+06	0.88018E-03 0.25697E-03	0.11459E-03 0.22425E+01	0.10247E-03 0.22428E+01	0.52500E-02 0.10629E-09	0.26576E-07 0.22970E-03	0.52191E+03 0.27000E+04
4	0.27331E+00 0.36670E-02	0.20057E+02 0.64319E+06	0.95406E-03 0.40458E-03	0.13162E-03 0.22276E+01	0.11097E-03 0.22282E+01	0.34102E-02 0.45796E-09	0.13784E-06 0.24697E-03	0.52255E+03 0.36000E+04
5	0.40030E+00 0.73690E-02	0.25574E+02 0.12011E+07	0.10784E-02 0.64631E-03	0.28746E-03 0.22484E+01	0.12578E-03 0.22489E+01	0.22873E-02 0.15226E-08	0.52327E-06 0.28245E-03	0.52306E+03 0.36000E+04
6	0.60524E+00 0.14809E-01	0.30706E+02 0.21803E+07	0.12914E-02 0.11170E-02	0.43731E-03 0.22922E+01	0.15365E-03 0.22928E+01	0.14721E-02 0.44767E-08	0.17162E-05 0.35182E-03	0.52362E+03 0.36000E+04
7	0.87623E+00 0.26135E-01	0.33894E+02 0.34841E+07	0.16085E-02 0.18473E-02	0.79077E-03 0.23361E+01	0.19254E-03 0.23367E+01	0.10008E-02 0.97227E-08	0.39893E-05 0.45011E-03	0.52438E+03 0.36000E+04
8	0.12089E+01 0.41155E-01	0.35583E+02 0.50469E+07	0.19532E-02 0.28507E-02	0.11983E-02 0.23790E+01	0.23934E-03 0.23797E+01	0.72064E-03 0.16807E-07	0.72319E-05 0.56937E-03	0.52523E+03 0.36000E+04
9	0.16597E+01 0.62414E-01	0.36579E+02 0.71217E+07	0.23945E-02 0.42639E-02	0.17690E-02 0.24104E+01	0.29740E-03 0.24112E+01	0.53705E-03 0.26350E-07	0.11823E-04 0.71721E-03	0.52631E+03 0.36000E+04
10	0.21774E+01 0.87458E-01	0.37018E+02 0.94547E+07	0.29024E-02 0.59220E-02	0.24294E-02 0.24376E+01	0.35380E-03 0.24385E+01	0.41938E-03 0.36729E-07	0.16983E-04 0.87439E-03	0.52743E+03 0.36000E+04
11	0.26875E+01 0.11243E+00	0.37156E+02 0.11714E+08	0.33549E-02 0.75450E-02	0.30738E-02 0.24546E+01	0.41553E-03 0.24556E+01	0.34934E-03 0.46199E-07	0.21800E-04 0.10201E-02	0.52847E+03 0.36000E+04

12	0.31937E+01	0.37163E+02	0.37752E-02	0.36993E-02	0.46904E-03	0.30045E-03	0.26279E-04	0.52942E+03
	0.13749E+00	0.13925E+08	0.91325E-02	0.24687E+01	0.24697E+01	0.54882E-07	0.11582E-02	0.36000E+04
13	0.36976E+01	0.37112E+02	0.41742E-02	0.+3059E-02	0.52042E-03	0.26506E-03	0.30425E-04	0.53032E+03
	0.16249E+00	0.16097E+08	0.10674E-01	0.24789E+01	0.24800E+01	0.62869E-07	0.12904E-02	0.36000E+04
14	0.42000E+01	0.37018E+02	0.45608E-02	0.48947E-02	0.57050E-03	0.23662E-03	0.34266E-04	0.53119E+03
	0.18749E+00	0.18233E+08	0.12184E-01	0.24892E+01	0.24904E+01	0.70230E-07	0.14205E-02	0.36000E+04
15	0.47015E+01	0.36900E+02	0.83922E-02	0.73927E-02	0.83791E-03	0.19356E-02	0.49771E-04	0.52236E+03
	0.21250E+00	0.20251E+08	0.10808E-01	0.14619E+01	0.14626E+01	0.10324E-06	0.12269E-02	0.36000E+04
16	0.52024E+01	0.36769E+02	0.15437E-01	0.12876E-01	0.14274E-02	0.28+65E-02	0.85351E-04	0.52011E+03
	0.23750E+00	0.22439E+08	0.16708E-01	0.12976E+01	0.12986E+01	0.17669E-06	0.18557E-02	0.0
17	0.57029E+01	0.36632E+02	0.20874E-01	0.18959E-01	0.20671E-02	0.26887E-02	0.12424E-03	0.52009E+03
	0.26250E+00	0.24506E+08	0.24890E-01	0.13128E+01	0.13138E+01	0.26251E-06	0.27218E-02	0.0
18	0.62032E+01	0.36493E+02	0.28222E-01	0.25276E-01	0.27209E-02	0.25594E-02	0.16353E-03	0.52003E+03
	0.28750E+00	0.26555E+08	0.32206E-01	0.12742E+01	0.12758E+01	0.34437E-06	0.34815E-02	0.0
19	0.67034E+01	0.36356E+02	0.35309E-01	0.31458E-01	0.33546E-02	0.24864E-02	0.20109E-03	0.52021E+03
	0.31250E+00	0.28588E+08	0.39611E-01	0.12592E+01	0.12608E+01	0.42325E-06	0.42455E-02	0.0
20	0.72034E+01	0.36226E+02	0.41939E-01	0.37512E-01	0.39737E-02	0.24802E-02	0.23710E-03	0.52006E+03
	0.33750E+00	0.30611E+08	0.47145E-01	0.12568E+01	0.12585E+01	0.50084E-06	0.50258E-02	0.0
21	0.77034E+01	0.36105E+02	0.48989E-01	0.43639E-01	0.46009E-02	0.23667E-02	0.27282E-03	0.52013E+03
	0.36250E+00	0.32627E+08	0.53378E-01	0.12232E+01	0.12262E+01	0.57637E-06	0.56686E-02	0.0
22	0.82034E+01	0.35999E+02	0.56694E-01	0.49681E-01	0.52214E-02	0.23741E-02	0.30777E-03	0.52006E+03
	0.38750E+00	0.34643E+08	0.60718E-01	0.12222E+01	0.12252E+01	0.64998E-06	0.64349E-02	0.0
23	0.87034E+01	0.35914E+02	0.63426E-01	0.55592E-01	0.58302E-02	0.22995E-02	0.34185E-03	0.52010E+03
	0.41250E+00	0.36667E+08	0.68007E-01	0.12233E+01	0.12264E+01	0.72226E-06	0.71996E-02	0.0
24	0.92034E+01	0.35864E+02	0.70912E-01	0.61225E-01	0.64116E-02	0.22878E-02	0.37487E-03	0.52007E+03
	0.43750E+00	0.38719E+08	0.74860E-01	0.12227E+01	0.12258E+01	0.79298E-06	0.79222E-02	0.0
25	0.97034E+01	0.35878E+02	0.76672E-01	0.66457E-01	0.69513E-02	0.22486E-02	0.40739E-03	0.52008E+03
	0.46250E+00	0.40839E+08	0.81168E-01	0.12214E+01	0.12246E+01	0.86284E-06	0.85872E-02	0.0
26	0.10203E+02	0.35954E+02	0.83619E-01	0.71254E-01	0.74473E-02	0.22485E-02	0.43967E-03	0.52006E+03
	0.48750E+00	0.43035E+08	0.86880E-01	0.12193E+01	0.12226E+01	0.93227E-06	0.91923E-02	0.0
27	0.10703E+02	0.36059E+02	0.89092E-01	0.75725E-01	0.79152E-02	0.22192E-02	0.47151E-03	0.52007E+03
	0.51250E+00	0.45276E+08	0.92190E-01	0.12174E+01	0.12208E+01	0.10015E-05	0.97633E-02	0.0
28	0.11203E+02	0.36176E+02	0.93827E-01	0.79970E-01	0.83716E-02	0.22177E-02	0.50294E-03	0.52006E+03
	0.53750E+00	0.47544E+08	0.97225E-01	0.12158E+01	0.12192E+01	0.10706E-05	0.10321E-01	0.0
29	0.11704E+02	0.36294E+02	0.98207E-01	0.84047E-01	0.88292E-02	0.21888E-02	0.53396E-03	0.52006E+03
	0.56250E+00	0.49823E+08	0.10209E+00	0.12147E+01	0.12183E+01	0.11394E-05	0.10886E-01	0.0
30	0.12204E+02	0.36406E+02	0.10323E+00	0.88001E-01	0.93005E-02	0.21819E-02	0.56446E-03	0.52006E+03
	0.58750E+00	0.52113E+08	0.10683E+00	0.12139E+01	0.12176E+01	0.12077E-05	0.11469E-01	0.0

BEST AVAILABLE COPY

31	0.12704E+02	0.36505E+02	0.10810E+00	0.91878E-01	0.97993E-02	0.21520E-02	0.59431E-03	0.52006E+03
	0.61250E+00	0.54402E+08	0.11151E+00	0.12137E+01	0.12175E+01	0.12752E-05	0.12095E-01	0.0
32	0.13204E+02	0.36583E+02	0.11307E+00	0.95720E-01	0.10341E-01	0.21388E-02	0.62330E-03	0.52006E+03
	0.63750E+00	0.54667E+08	0.11618E+00	0.12137E+01	0.12177E+01	0.13416E-05	0.12778E-01	0.0
33	0.13705E+02	0.36634E+02	0.11836E+00	0.99577E-01	0.10946E-01	0.21058E-02	0.65122E-03	0.52005E+03
	0.66250E+00	0.58697E+08	0.12092E+00	0.12143E+01	0.12185E+01	0.14064E-05	0.13550E-01	0.0
34	0.14206E+02	0.36649E+02	0.12420E+00	0.10351E+00	0.11638E-01	0.20838E-02	0.67783E-03	0.52006E+03
	0.68750E+00	0.61076E+08	0.12580E+00	0.12153E+01	0.12197E+01	0.14691E-05	0.14441E-01	0.0
35	0.14708E+02	0.36620E+02	0.13084E+00	0.10759E+00	0.12448E-01	0.20441E-02	0.70283E-03	0.52005E+03
	0.71250E+00	0.63183E+08	0.13094E+00	0.12171E+01	0.12218E+01	0.15291E-05	0.15499E-01	0.0
36	0.15211E+02	0.36537E+02	0.14274E+00	0.11259E+00	0.13497E-01	0.20156E-02	0.72984E-03	0.52005E+03
	0.73751E+00	0.65195E+08	0.13340E+00	0.11849E+01	0.11934E+01	0.15860E-05	0.16409E-01	0.0
37	0.15714E+02	0.36391E+02	0.15810E+00	0.11810E+00	0.14794E-01	0.19646E-02	0.75619E-03	0.52005E+03
	0.76251E+00	0.67085E+08	0.14028E+00	0.11878E+01	0.11972E+01	0.16390E-05	0.18096E-01	0.0
38	0.16220E+02	0.36169E+02	0.17706E+00	0.12424E+00	0.16425E-01	0.19094E-02	0.78061E-03	0.52005E+03
	0.78751E+00	0.68818E+08	0.14805E+00	0.11916E+01	0.12020E+01	0.16874E-05	0.20253E-01	0.0
39	0.16720E+02	0.35853E+02	0.19795E+00	0.13126E+00	0.18540E-01	0.18506E-02	0.80298E-03	0.52005E+03
	0.81251E+00	0.70357E+08	0.15710E+00	0.11969E+01	0.12087E+01	0.17307E-05	0.23111E-01	0.0
40	0.17235E+02	0.35440E+02	0.22435E+00	0.13952E+00	0.21369E-01	0.17698E-02	0.82316E-03	0.52005E+03
	0.83752E+00	0.71657E+08	0.15801E+00	0.12042E+01	0.12181E+01	0.17684E-05	0.27047E-01	0.0
41	0.17747E+02	0.34896E+02	0.26196E+00	0.14961E+00	0.25311E-01	0.16725E-02	0.84133E-03	0.52005E+03
	0.86252E+00	0.72651E+08	0.18172E+00	0.12146E+01	0.12315E+01	0.17998E-05	0.32749E-01	0.0
42	0.18262E+02	0.34196E+02	0.30914E+00	0.16255E+00	0.31086E-01	0.15358E-02	0.85813E-03	0.52005E+03
	0.88752E+00	0.73260E+08	0.19938E+00	0.12296E+01	0.12514E+01	0.18245E-05	0.41579E-01	0.0
43	0.18780E+02	0.33295E+02	0.37876E+00	0.18038E+00	0.40150E-01	0.13574E-02	0.87581E-03	0.52004E+03
	0.91253E+00	0.73356E+08	0.22602E+00	0.12530E+01	0.12833E+01	0.18425E-05	0.56629E-01	0.0
44	0.19303E+02	0.32114E+02	0.48089E+00	0.20857E+00	0.55930E-01	0.10709E-02	0.90289E-03	0.52004E+03
	0.93753E+00	0.72725E+08	0.27018E+00	0.12954E+01	0.13436E+01	0.18538E-05	0.86579E-01	0.0
45	0.19831E+02	0.30451E+02	0.63586E+00	0.27306E+00	0.89839E-01	0.47556E-03	0.99129E-03	0.52004E+03
	0.96253E+00	0.70845E+08	0.38742E+00	0.14188E+01	0.15281E+01	0.18588E-05	0.16850E+00	0.0

BEST AVAILABLE COPY

The third sample case is similar to the second one except that the working fluid is sea water (KN=3) and calculations for the heated portion of the body were done with the wall temperature specified at a constant 540°R. The surface temperature was assumed to vary linearly from its specified value on the heated portion to the freestream value on the rest of the body. Summary of the input data is presented below. Profile data at station 14 near 19-percent chord location is added to show the effect of heating on a laminar profile. Although the local pressure gradient is slightly adverse, the two-dimensional shape parameter H_2 from the summary page shows that the profile effectively corresponds to one obtainable in a slightly favorable pressure gradient with no heating.

BODY 5A IN WATWR, WALL TEMP. SPEC.

BEST AVAILABLE COPY

** CASE DATA

NXT	= 46	NTR	= 15	KN	= 3		
IWALL	= 1	ISFD	= 0	NXY	= 46		
ETAE	= 0.600000E+01	DETA1	= 0.100000E-02	VGP	= 0.114000E+01	CL	= 0.200000E+02
UFRS	= 0.350000E+02	TFRS	= 0.520000E+03	PFRS	= 0.125393E+04		
RHOFRS	= 0.199026E+01	PRFRS	= 0.823630E+01	RMUI	= 0.250079E-04	RCI	= 0.200000E+07

** STATION DATA

NX	X	RC	UE	HTP		BV	P2
1	0.0	0.0	0.0	0.540000E+03	0.0		0.333333E+00
2	0.700318E-01	0.349200E-02	0.597502E+01	0.540000E+03	0.0		0.479140E+00
3	0.181736E+00	0.889500E-02	0.144737E+02	0.540000E+03	0.0		0.327130E+00
4	0.273307E+00	0.130170E-01	0.200569E+02	0.540000E+03	0.0		0.266799E+00
5	0.400303E+00	0.181760E-01	0.255738E+02	0.540000E+03	0.0		0.209588E+00
6	0.605241E+00	0.252220E-01	0.307059E+02	0.540000E+03	0.0		0.146102E+00
7	0.876230E+00	0.326590E-01	0.338938E+02	0.540000E+03	0.0		0.917816E-01
8	0.120895E+01	0.398110E-01	0.355877E+02	0.540000E+03	0.0		0.561246E-01
9	0.165969E+01	0.472930E-01	0.365788E+02	0.540000E+03	0.0		0.322511E-01
10	0.217736E+01	0.538310E-01	0.370175E+02	0.540000E+03	0.0		0.156481E-01
11	0.266754E+01	0.588070E-01	0.371563E+02	0.540000E+03	0.0		0.531347E-02
12	0.319373E+01	0.626960E-01	0.371683E+02	0.540000E+03	0.0		-0.195345E-02
13	0.369758E+01	0.657670E-01	0.371123E+02	0.540000E+03	0.0		-0.801672E-02
14	0.419999E+01	0.681920E-01	0.370175E+02	0.540000E+03	0.0		-0.133215E-01
15	0.470148E+01	0.700960E-01	0.368999E+02	0.540000E+03	0.0		-0.180987E-01
16	0.520239E+01	0.715730E-01	0.367690E+02	0.535000E+03	0.0		-0.223988E-01
17	0.570291E+01	0.726970E-01	0.366316E+02	0.530000E+03	0.0		-0.261743E-01
18	0.620319E+01	0.735310E-01	0.364926E+02	0.525000E+03	0.0		-0.293441E-01
19	0.670335E+01	0.741260E-01	0.363561E+02	0.520000E+03	0.0		-0.317452E-01
20	0.720341E+01	0.745290E-01	0.362256E+02	0.520000E+03	0.0		-0.330622E-01
21	0.770344E+01	0.747820E-01	0.361052E+02	0.520000E+03	0.0		-0.328529E-01
22	0.820345E+01	0.749210E-01	0.359992E+02	0.520000E+03	0.0		-0.303174E-01
23	0.870345E+01	0.749830E-01	0.359138E+02	0.520000E+03	0.0		-0.232297E-01
24	0.920345E+01	0.750000E-01	0.358638E+02	0.520000E+03	0.0		-0.650577E-02
25	0.970345E+01	0.749990E-01	0.358779E+02	0.520000E+03	0.0		0.182705E-01
26	0.102034E+02	0.749750E-01	0.359539E+02	0.520000E+03	0.0		0.391323E-01
27	0.107035E+02	0.748900E-01	0.360593E+02	0.520000E+03	0.0		0.510035E-01
28	0.112035E+02	0.746980E-01	0.361757E+02	0.520000E+03	0.0		0.572916E-01
29	0.117035E+02	0.743580E-01	0.362939E+02	0.520000E+03	0.0		0.597221E-01
30	0.122036E+02	0.738280E-01	0.364060E+02	0.520000E+03	0.0		0.580343E-01
31	0.127039E+02	0.730650E-01	0.365048E+02	0.520000E+03	0.0		0.522920E-01
32	0.132043E+02	0.720280E-01	0.365833E+02	0.520000E+03	0.0		0.408520E-01
33	0.137051E+02	0.706740E-01	0.366340E+02	0.520000E+03	0.0		0.230363E-01
34	0.142063E+02	0.689610E-01	0.366490E+02	0.520000E+03	0.0		-0.519674E-02
35	0.147081E+02	0.668460E-01	0.366199E+02	0.520000E+03	0.0		-0.449742E-01

36	0.152107E+02	0.642870E-01	0.365374E+02	0.520000E+03	0.0	-0.103579E+00
37	0.157144E+02	0.612420E-01	0.363911E+02	0.520000E+03	0.0	-0.190353E+00
38	0.162196E+02	0.576680E-01	0.361691E+02	0.520000E+03	0.0	-0.319893E+00
39	0.167264E+02	0.535240E-01	0.358578E+02	0.520000E+03	0.0	-0.520694E+00
40	0.172355E+02	0.487670E-01	0.354404E+02	0.520000E+03	0.0	-0.848496E+00
41	0.177471E+02	0.433550E-01	0.348961E+02	0.520000E+03	0.0	-0.142302E+01
+2	0.182619E+02	0.372450E-01	0.341959E+02	0.520000E+03	0.0	-0.254137E+01
43	0.187804E+02	0.303950E-01	0.332953E+02	0.520000E+03	0.0	-0.509481E+01
44	0.193032E+02	0.227630E-01	0.321142E+02	0.520000E+03	0.0	-0.128093E+02
+5	0.198311E+02	0.143060E-01	0.304507E+02	0.520000E+03	0.0	-0.531136E+02
46	0.203649E+02	0.498300E-02	0.276568E+02	0.520000E+03	0.0	-0.723739E+03

NX= 14 X= 0.42000E+01 XB= 0.10836E-01

V(1,2)= 0.424152E+00 DELV(1)= -0.131671E-01

V(1,2)= 0.410986E+00 DELV(1)= -0.520334E-03

V(1,2)= 0.410465E+00 DELV(1)= -0.639089E-04

J	ETA	U	V	W	T	TEMP	Y
1	0.0	0.0	0.410401E+00	0.104022E+01	-0.281081E-01	0.539999E+03	0.0
5	0.00492	0.201934E-02	0.410330E+00	0.104008E+01	-0.281448E-01	0.539927E+03	0.441619E-05
9	0.01323	0.542805E-02	0.409870E+00	0.103984E+01	-0.281413E-01	0.539806E+03	0.118748E-04
13	0.02727	0.111767E-01	0.409103E+00	0.103945E+01	-0.281258E-01	0.539601E+03	0.244716E-04
17	0.05095	0.208621E-01	0.407843E+00	0.103878E+01	-0.281438E-01	0.539255E+03	0.457459E-04
21	0.09103	0.371501E-01	0.405693E+00	0.103766E+01	-0.281323E-01	0.538670E+03	0.816736E-04
25	0.15866	0.644524E-01	0.401696E+00	0.103575E+01	-0.281208E-01	0.537682E+03	0.142344E-03
29	0.27289	0.109987E+00	0.395343E+00	0.103254E+01	-0.280503E-01	0.536015E+03	0.244783E-03
33	0.46582	0.185125E+00	0.383246E+00	0.102717E+01	-0.275490E-01	0.533226E+03	0.417718E-03
37	0.79166	0.306351E+00	0.360119E+00	0.101854E+01	-0.250161E-01	0.528746E+03	0.709580E-03
41	1.34203	0.491928E+00	0.313492E+00	0.100716E+01	-0.154973E-01	0.522834E+03	0.120200E-02
45	2.27156	0.742106E+00	0.221660E+00	0.100037E+01	-0.154367E-02	0.519296E+03	0.203273E-02
49	3.84149	0.957112E+00	0.613728E-01	0.999999E+00	0.278877E-05	0.519095E+03	0.343443E-02
53	6.49306	0.999919E+00	0.196260E-03	0.100000E+01	-0.708327E-06	0.519093E+03	0.579858E-02
56	9.62320	0.100000E+01	-0.725481E-06	0.100000E+01	-0.219688E-06	0.519093E+03	0.858422E-02

BEST AVAILABLE COPY

BEST AVAILABLE COPY

OUTPUT SUMMARY

NX	X X/C	UE RX	DEL DISPA	MOMA HA	MOM2 H2	CF CFT	CD DISPLT	TW QW
1	0.0 0.0	0.0 0.0	0.80660E-03 0.0	0.0 0.0	0.91523E-04 0.22006E+01	0.0 0.0	0.0 0.20141E-03	0.54000E+03 0.31462E+05
2	0.70032E-01 0.25900E-03	0.59750E+01 0.32912E+05	0.91393E-03 0.97590E-04	0.45120E-04 0.21629E+01	0.10279E-03 0.21632E+01	0.12659E-01 0.26209E-11	0.39986E-09 0.22150E-03	0.54000E+03 0.27459E+05
3	0.18174E+00 0.16740E-02	0.14474E+02 0.20689E+06	0.85462E-03 0.24087E-03	0.10896E-03 0.22106E+01	0.97442E-04 0.22109E+01	0.51350E-02 0.10376E-09	0.22481E-07 0.21496E-03	0.54000E+03 0.28778E+05
4	0.27331E+00 0.36670E-02	0.20057E+02 0.43103E+06	0.93269E-03 0.39347E-03	0.17631E-03 0.22317E+01	0.10773E-03 0.22321E+01	0.32894E-02 0.44615E-09	0.11724E-06 0.24013E-03	0.54000E+03 0.26888E+05
5	0.40030E+00 0.73690E-02	0.25574E+02 0.80481E+06	0.10376E-02 0.62568E-03	0.27906E-03 0.22421E+01	0.12211E-03 0.22425E+01	0.22342E-02 0.14855E-08	0.44603E-06 0.27353E-03	0.54000E+03 0.24146E+05
6	0.60524E+00 0.14809E-01	0.30706E+02 0.14606E+07	0.12777E-02 0.10859E-02	0.47579E-03 0.22823E+01	0.15002E-03 0.22828E+01	0.14372E-02 0.43830E-08	0.14707E-05 0.34255E-03	0.54000E+03 0.19936E+05
7	0.87623E+00 0.26135E-01	0.33894E+02 0.23337E+07	0.15717E-02 0.17956E-02	0.77534E-03 0.23159E+01	0.18879E-03 0.23164E+01	0.98818E-03 0.95576E-08	0.34320E-05 0.43744E-03	0.54000E+03 0.16140E+05
8	0.12089E+01 0.41155E-01	0.35588E+02 0.32818E+07	0.19420E-02 0.27811E-02	0.11798E-02 0.23573E+01	0.23564E-03 0.23580E+01	0.71289E-03 0.16590E-07	0.62441E-05 0.55508E-03	0.54000E+03 0.13071E+05
9	0.16597E+01 0.62414E-01	0.36579E+02 0.47705E+07	0.24102E-02 0.41704E-02	0.17479E-02 0.23859E+01	0.29387E-03 0.23866E+01	0.53629E-03 0.26116E-07	0.10241E-04 0.70095E-03	0.54000E+03 0.10638E+05
10	0.21774E+01 0.87458E-01	0.37013E+02 0.63395E+07	0.28887E-02 0.58160E-02	0.24081E-02 0.24152E+01	0.35565E-03 0.24160E+01	0.41988E-03 0.36539E-07	0.14756E-04 0.85954E-03	0.54000E+03 0.88459E+04
11	0.26875E+01 0.11248E+00	0.37156E+02 0.78542E+07	0.33257E-02 0.74337E-02	0.30560E-02 0.24325E+01	0.41313E-03 0.24333E+01	0.35217E-03 0.46094E-07	0.18998E-04 0.10052E-02	0.54000E+03 0.76766E+04
12	0.31937E+01 0.13749E+00	0.37168E+02 0.93366E+07	0.37332E-02 0.90319E-02	0.36869E-02 0.24497E+01	0.46747E-03 0.24506E+01	0.30327E-03 0.54392E-07	0.22960E-04 0.11461E-02	0.54000E+03 0.68017E+04
13	0.36976E+01 0.16249E+00	0.37112E+02 0.10793E+08	0.41355E-02 0.10586E-01	0.43000E-02 0.24619E+01	0.51971E-03 0.24628E+01	0.26889E-03 0.63008E-07	0.26637E-04 0.12803E-02	0.54000E+03 0.61434E+04
14	0.42000E+01 0.18749E+00	0.37013E+02 0.12223E+08	0.45640E-02 0.12121E-01	0.48965E-02 0.24755E+01	0.57071E-03 0.24765E+01	0.24037E-03 0.70514E-07	0.30056E-04 0.14126E-02	0.54000E+03 0.55971E+04
15	0.47015E+01 0.21250E+00	0.36900E+02 0.13630E+08	0.78735E-02 0.10973E-01	0.70839E-02 0.15491E+01	0.80297E-03 0.15496E+01	0.16484E-02 0.99338E-07	0.41929E-04 0.12456E-02	0.54000E+03 0.63196E+05
16	0.52024E+01 0.23750E+00	0.36709E+02 0.15029E+08	0.14529E-01 0.16491E-01	0.12047E-01 0.13689E+01	0.13357E-02 0.13695E+01	0.26541E-02 0.16573E-06	0.70169E-04 0.18325E-02	0.53500E+03 0.75408E+05
17	0.57029E+01 0.26250E+00	0.36632E+02 0.16413E+08	0.21830E-01 0.24397E-01	0.18273E-01 0.13351E+01	0.19921E-02 0.13359E+01	0.26687E-02 0.24864E-06	0.10509E-03 0.26677E-02	0.53000E+03 0.47625E+05

18	0.62032E+01	0.36493E+02	0.28772E-01	0.24674E-01	0.26558E-02	0.26450E-02	0.14016E-03	0.52500E+03
	0.23750E+00	0.17788E+08	0.32574E-01	0.13202E+01	0.13212E+01	0.33189E-06	0.35208E-02	0.23327E+05
19	0.67034E+01	0.36356E+02	0.35364E-01	0.30885E-01	0.32938E-02	0.25004E-02	0.17339E-03	0.52500E+03
	0.31250E+00	0.19150E+08	0.40859E-01	0.13229E+01	0.13241E+01	0.41268E-06	0.43799E-02	-0.27574E+04
20	0.72034E+01	0.36226E+02	0.42428E-01	0.37069E-01	0.39269E-02	0.24475E-02	0.20573E-03	0.52000E+03
	0.35750E+00	0.20518E+08	0.48811E-01	0.13168E+01	0.13181E+01	0.49033E-06	0.52020E-02	0.39981E+03
21	0.77034E+01	0.36105E+02	0.49411E-01	0.43138E-01	0.45484E-02	0.23854E-02	0.23687E-03	0.52000E+03
	0.36250E+00	0.21869E+08	0.56367E-01	0.13067E+01	0.13081E+01	0.56597E-06	0.59853E-02	0.15449E+03
22	0.82034E+01	0.35999E+02	0.55701E-01	0.49031E-01	0.51540E-02	0.23692E-02	0.26672E-03	0.52000E+03
	0.38750E+00	0.23220E+08	0.63752E-01	0.13002E+01	0.13018E+01	0.64012E-06	0.67564E-02	0.13380E+04
23	0.87034E+01	0.35914E+02	0.60884E-01	0.54641E-01	0.57325E-02	0.23124E-02	0.29501E-03	0.52000E+03
	0.41250E+00	0.24573E+08	0.70893E-01	0.12974E+01	0.12992E+01	0.71285E-06	0.75042E-02	0.12228E+04
24	0.92034E+01	0.35864E+02	0.67638E-01	0.60286E-01	0.63151E-02	0.22926E-02	0.32405E-03	0.52000E+03
	0.43750E+00	0.25949E+08	0.77930E-01	0.12927E+01	0.12946E+01	0.78415E-06	0.82455E-02	0.17670E+04
25	0.97034E+01	0.35878E+02	0.75044E-01	0.65593E-01	0.68626E-02	0.22597E-02	0.35299E-03	0.52000E+03
	0.46250E+00	0.27369E+08	0.84468E-01	0.12878E+01	0.12898E+01	0.85457E-06	0.89348E-02	0.17754E+04
26	0.10203E+02	0.35954E+02	0.81914E-01	0.70495E-01	0.73690E-02	0.22476E-02	0.38188E-03	0.52000E+03
	0.48750E+00	0.28841E+08	0.90425E-01	0.12827E+01	0.12849E+01	0.92446E-06	0.95669E-02	0.20367E+04
27	0.10703E+02	0.36052E+02	0.87449E-01	0.75102E-01	0.78505E-02	0.22275E-02	0.41056E-03	0.52000E+03
	0.51250E+00	0.30347E+08	0.95981E-01	0.12780E+01	0.12803E+01	0.99415E-06	0.10163E-01	0.21154E+04
28	0.11203E+02	0.36176E+02	0.94770E-01	0.79533E-01	0.83254E-02	0.22187E-02	0.43917E-03	0.52000E+03
	0.53750E+00	0.31863E+08	0.10133E+00	0.12740E+01	0.12765E+01	0.10637E-05	0.10756E-01	0.22350E+04
29	0.11704E+02	0.36294E+02	0.10111E+00	0.83839E-01	0.88057E-02	0.21958E-02	0.46768E-03	0.52000E+03
	0.56250E+00	0.33399E+08	0.10652E+00	0.12706E+01	0.12732E+01	0.11329E-05	0.11356E-01	0.23416E+04
30	0.12204E+02	0.36405E+02	0.10701E+00	0.88094E-01	0.93070E-02	0.21855E-02	0.49617E-03	0.52000E+03
	0.58750E+00	0.34911E+08	0.11169E+00	0.12677E+01	0.12705E+01	0.12017E-05	0.11988E-01	0.23832E+04
31	0.12704E+02	0.36505E+02	0.11336E+00	0.92285E-01	0.98377E-02	0.21591E-02	0.52418E-03	0.52000E+03
	0.61250E+00	0.36441E+08	0.11678E+00	0.12654E+01	0.12683E+01	0.12697E-05	0.12664E-01	0.24902E+04
32	0.13204E+02	0.36583E+02	0.12110E+00	0.96484E-01	0.10417E-01	0.21438E-02	0.55170E-03	0.52000E+03
	0.63750E+00	0.37958E+08	0.12191E+00	0.12635E+01	0.12666E+01	0.13365E-05	0.13406E-01	0.24884E+04
33	0.13705E+02	0.36634E+02	0.12879E+00	0.10075E+00	0.11065E-01	0.21124E-02	0.57858E-03	0.52000E+03
	0.66250E+00	0.39446E+08	0.12717E+00	0.12622E+01	0.12655E+01	0.14017E-05	0.14246E-01	0.25801E+04
34	0.14206E+02	0.36649E+02	0.13684E+00	0.10513E+00	0.11807E-01	0.20899E-02	0.60451E-03	0.52000E+03
	0.68750E+00	0.40905E+08	0.13260E+00	0.12613E+01	0.12649E+01	0.14649E-05	0.15217E-01	0.25520E+04
35	0.14708E+02	0.36620E+02	0.14563E+00	0.10971E+00	0.12676E-01	0.20511E-02	0.62928E-03	0.52000E+03
	0.71250E+00	0.42317E+08	0.13835E+00	0.12610E+01	0.12650E+01	0.15254E-05	0.16369E-01	0.26173E+04
36	0.15211E+02	0.36537E+02	0.15555E+00	0.11457E+00	0.13717E-01	0.20175E-02	0.65254E-03	0.52000E+03
	0.73751E+00	0.43671E+08	0.14452E+00	0.12613E+01	0.12657E+01	0.15826E-05	0.17766E-01	0.25729E+04

BEST AVAILABLE COPY

37	0.15714E+02	0.36391E+02	0.16775E+00	0.11987E+00	0.14997E-01	0.19728E-02	0.67418E-03	0.52000E+03
	0.76251E+00	0.44937E+08	0.15133E+00	0.12625E+01	0.12674E+01	0.16360E-05	0.19509E-01	0.25947E+04
38	0.16220E+02	0.36169E+02	0.18258E+00	0.12571E+00	0.16603E-01	0.19195E-02	0.69364E-03	0.52000E+03
	0.78751E+00	0.46127E+08	0.15898E+00	0.12647E+01	0.12703E+01	0.16849E-05	0.21736E-01	0.25373E+04
39	0.16726E+02	0.35858E+02	0.20042E+00	0.13241E+00	0.18689E-01	0.19525E-02	0.71114E-03	0.52000E+03
	0.81251E+00	0.47152E+08	0.16792E+00	0.12681E+01	0.12748E+01	0.17286E-05	0.24684E-01	0.25128E+04
40	0.17235E+02	0.35440E+02	0.22249E+00	0.14028E+00	0.21478E-01	0.17769E-02	0.72627E-03	0.52000E+03
	0.83752E+00	0.48014E+08	0.17863E+00	0.12734E+01	0.12816E+01	0.17665E-05	0.28733E-01	0.24224E+04
41	0.17747E+02	0.34896E+02	0.25711E+00	0.15059E+00	0.25461E-01	0.16721E-02	0.74269E-03	0.52000E+03
	0.86252E+00	0.48672E+08	0.19279E+00	0.12803E+01	0.12911E+01	0.17981E-05	0.34708E-01	0.23483E+04
42	0.18262E+02	0.34196E+02	0.30618E+00	0.16379E+00	0.31295E-01	0.15368E-02	0.75790E-03	0.52000E+03
	0.88752E+00	0.49118E+08	0.21147E+00	0.12912E+01	0.13062E+01	0.18229E-05	0.43925E-01	0.22087E+04
43	0.18780E+02	0.33295E+02	0.37775E+00	0.18220E+00	0.40484E-01	0.13553E-02	0.77485E-03	0.52000E+03
	0.91253E+00	0.49166E+08	0.23855E+00	0.13093E+01	0.13323E+01	0.18410E-05	0.59634E-01	0.20329E+04
44	0.19303E+02	0.32114E+02	0.48550E+00	0.21149E+00	0.56508E-01	0.10658E-02	0.80137E-03	0.52000E+03
	0.93753E+00	0.48742E+08	0.28441E+00	0.13448E+01	0.13855E+01	0.18523E-05	0.90772E-01	0.17573E+04
45	0.19831E+02	0.30451E+02	0.67775E+00	0.28003E+00	0.91208E-01	0.46156E-03	0.88945E-03	0.52000E+03
	0.96253E+00	0.47452E+08	0.40744E+00	0.14550E+01	0.15598E+01	0.18573E-05	0.17560E+00	0.11790E+04

BEST AVAILABLE COPY

4. STANDARD AND INVERSE POTENTIAL-FLOW METHOD

The standard and inverse potential-flow solution procedure is based on the analytical method of James[3]. This method, originally developed for shapes having either a cusped or blunt trailing edge, has been extended to include trailing edges of arbitrary angle. It is based on a mapping of the body shape to a unit circle. This mapping can be performed either analytically if the mapping function is known, or numerically through a program which determines the Fourier coefficients of the mapping. Once this is accomplished the surface coordinate of the body is expressed as an expansion in the circle plane, which allows the solution to the governing equation to be expressed as sequence of solutions to recursively generated equations. This permits an arbitrary number of terms to be generated depending on the accuracy desired. The details of this procedure are outlined below, and a description of the computer program is included in Section 5.0.

4.1 Equations of Motion

This section deals with the development of a general analysis method for axisymmetric flow very briefly. For more details, the reader should consult ref.. 3.

For an axisymmetric body lying in the (x,y)-plane such that the free-stream at infinity is parallel to the axis of symmetry (x), the velocity potential (ϕ) satisfies the well-known differential equation

$$\frac{\partial}{\partial x}\left(y\,\frac{\partial \phi}{\partial x}\right) + \frac{\partial}{\partial y}\left(y\,\frac{\partial \phi}{\partial y}\right) = 0 \qquad (4.1)$$

with the additional conditions that $\phi \sim x$ in the far field and that the derivative of ϕ normal to the profile vanishes on the profile. It is quite standard to seek orthogonal curvilinear transformations $x = x(\xi_1,\xi_2)$, $y = y(\xi_1,\xi_2)$ in order to either simplify (4.1) or the profile representation (thus making the normal derivative condition more tractable). Such a transformation leads to

$$\frac{\partial}{\partial \xi_1}\left(\frac{h_2}{h_1}\,y\,\frac{\partial \phi}{\partial \xi_1}\right) + \frac{\partial}{\partial \xi_2}\left(\frac{h_1}{h_2}\,y\,\frac{\partial \phi}{\partial \xi_2}\right) = 0 \qquad (4.2)$$

where h_1 and h_2 are the usual metrics, viz.

$$h_1 = \sqrt{\left(\frac{\partial x}{\partial \xi_1}\right)^2 + \left(\frac{\partial y}{\partial \xi_1}\right)^2}, \qquad h_2 = \sqrt{\left(\frac{\partial x}{\partial \xi_2}\right)^2 + \left(\frac{\partial y}{\partial \xi_2}\right)^2}$$

However, if the transformation is in particular a conformal mapping from the $\xi_1 + i\xi_2$-plane to the $x + iy$ plane, then the Cauchy-Riemann equations hold, that is

$$\frac{\partial x}{\partial \xi_1} = \frac{\partial y}{\partial \xi_2}, \qquad \frac{\partial x}{\partial \xi_2} = -\frac{\partial y}{\partial \xi_1}$$

and therefore, $h_1 = h_2$ which reduces (4.2) to

$$\frac{\partial}{\partial \xi_1}\left(y \frac{\partial \phi}{\partial \xi_1}\right) + \frac{\partial}{\partial \xi_2}\left(y \frac{\partial \phi}{\partial \xi_2}\right) = 0 \qquad (4.3)$$

Even though (4.3) is formally no simpler than (4.1), it is possible to find general mappings which greatly simplify the surface boundary condition by relating the given profile to one of a number of canonical forms in an auxiliary (ξ_1,ξ_2)-plane. Specifically, the class of mappings which map airfoil-like profiles into the unit circle have been found to be of great utility in two dimensions and so are considered further for this application.

4.2 Unit Circle Mapping

According to Riemann's fundamental mapping theorem, any profile whose contour encloses a singly-connected domain (in the usual engineering sense of, e.g., Woods[6]) can be mapped into the unit circle. However, for airfoils and axisymmetric bodies of interest to engineering, the types of mapping of sufficient generality and simplicity to be useful are quite constrained. The role of these constraints has been discussed by James[7] and need not be elaborated in detail here. Briefly, the desired characteristics are that: (a) the mapping should reflect the existence of a finite trailing-edge angle discontinuity $(\pi - \tau)$, (b) the mapping derivative must $\to 1$ as $|z| \to \infty$, (c) the profile must be closed, and (d) the mapping derivative must have neither zeros nor singularities on* or outside the unit circle.

*In the general theory of mapping methods, certain boundary singularities may arise, but they are not of interest in this application.

Let $\zeta = \xi + i\eta$ be the unit circle plane then it is easy to show that a mapping which conforms to (a) - (d) is of the type

$$\frac{dz}{d\zeta} = \left(1 - \frac{1}{\zeta}\right)^{1-\tau/\pi} g(\zeta) \tag{4.4}$$

where $g(\zeta)$ is an analytic function with neither zeros nor singularities outside C (the unit circle) and which $\to 1$ as $|\zeta| \to \infty$. Many different forms of $g(\zeta)$ can be used to generate profiles, but for the present purpose the more general representation of $g(\zeta)$ as an expansion

$$g(\zeta) = 1 + \frac{(1 - \tau/\pi)}{\zeta} + \frac{a_2}{\zeta^2} + \ldots \tag{4.5}$$

Note that the first coefficient a_1 is given by $a_1 = 1 - \tau/\pi$ because of the closure condition.

Now y is required in (4.3) and is described in (4.4) as the imaginary part of z. It can be shown that z is governed by a factor of the form $\zeta(1 - 1/\zeta)^{2-\tau/\pi}$, and direct inclusion of this into the differential equation would be desirable. However, an analytical solution under these circumstances has not been found. An alternative simpler procedure is to expand (4.4) and (4.5) to give

$$z = C + \zeta - \frac{B_1}{\zeta} - \frac{B_2}{\zeta^2} \ldots \tag{4.6}$$

for all values of τ. The convergence of (4.6) is guaranteed when $\tau = \pi$ or $\tau = 0$ because of the convergence of the a_n coefficients — which is in turn guaranteed by the theory (see ref. 7). For arbitrary τ $(0 \leq \tau \leq \pi)$ it might be expected that poor convergence could be a feature very close to the trailing edge, but experience has shown (see ref. 3 and the results quoted later) that this is not an important consideration with the kinds of bodies and term numbers of interest to this work. Moreover, this is not a subject to be pursued in detail in this report. Accepting that (4.6) is sufficient, it is clear that the B_n coefficients can be calculated readily from the a_n coefficients and the expansion for the singular factor in (4.4). On the other hand, if only a body shape is given, there are mapping programs available to find the a_n coefficients. The programs associated with this theory contain a subroutine option of this type.

With regard to the choice of variables in mapping from the unit circle it should be noted that the natural group $\zeta = re^{i\omega}$ is such that z is not an analytic function of $r + i\omega$ so that it is necessary to work with $\zeta = e^{\sigma}$, $\sigma = \lambda + i\omega$, $\tau = e^{\lambda}$. Then for axisymmetric bodies, the reflection symmetry ensures that all the a_n, B_n coefficients are real giving, from (4.6),

$$y = e^{\lambda} \sin\omega + B_1 e^{-\lambda} \sin\omega + B_2 e^{-2\lambda} \sin 2\omega + \ldots \tag{4.7}$$

to be used in the differential equation

$$\frac{\partial}{\partial\lambda}\left(y \frac{\partial\phi}{\partial\lambda}\right) + \frac{\partial}{\partial\omega}\left(y \frac{\partial\phi}{\partial\omega}\right) = 0 \tag{4.8}$$

with the conditions

$$\phi \sim e^{\lambda} \cos\omega \qquad \text{when} \qquad \lambda \to \infty \tag{4.9}$$

$$\frac{\partial\phi}{\partial\lambda} = 0 \qquad \text{when} \qquad \lambda = 0 \tag{4.10}$$

Although this is a properly posed problem which has so far defied analytic solution, the reduction presented here is by no means exhaustive; it is merely the simplest.

4.3 Method of Solution

The structure of y (eq. 4.8) suggests a scheme of solution in which ϕ is computed from a sequence of potentials ϕ_n sensitive to $\sin n\omega$ at each stage. An endless variety of such schemes exist, e.g., Kaplan[8]. His procedure is both elegant and complicated. Too complicated, in fact, to proceed either algebraically or automatically beyond the $\sin 3\omega$ term. From this, one rather obvious inference is that if the scheme is to be reducible to automatic computation of coefficients (as required to substantiate any claim of generality or analyticity) then each successive potential or function must not be governed by another partial-differential equation — and not even by an ordinary differential equation unless it can be solved directly in terms of known functions. With this understanding the natural choice for ϕ (an even periodic function) would be

$$\phi = f_0(\lambda) + f_1(\lambda) \cos\omega + f_2(\lambda) \cos 2\omega + \ldots$$

or perhaps, using $\xi = \cos\omega$, $\eta = e^{\lambda}$,

$$\phi = g_0(\eta) + g_1(\eta)\xi + g_2(\eta)\xi^2 + \ldots$$

However, these lead to systems of equations with strong coupling between the n-th function and <u>higher</u> order functions not yet known.

It turns out that the format which works in the sense that all coupling between equations is to <u>lower</u> order known functions is

$$\phi = \eta F_0(\xi) + \frac{1}{\eta} F_1(\xi) + \frac{1}{\eta^2} F_2(\xi) + \ldots \tag{4.11}$$

and this is the central feature of the whole theory. To go with (4.11) the $\sin\omega$ factor in y is removed reexpressing (4.7) as $y = \sin\omega \cdot Y(\xi,\eta)$ where

$$Y(\xi,\eta) = \eta + \frac{B_1}{\eta} + \frac{B_2}{\eta^2} U_1(\xi) + \ldots$$

and $U_n(\xi)$ is the Chebyshev polynomial of second kind. At the same time the differential equation becomes

$$Y\{\nabla^2\phi - \xi\phi_\xi\} + \eta^2 Y_\eta \phi_\eta + (1 - \xi^2) Y_\xi \phi_\xi = 0 \tag{4.12}$$

with the conditions

$$\begin{aligned} \phi_\eta &= 0 \qquad \text{when} \qquad \eta = 1 \\ \phi &\sim \xi\eta \qquad \text{when} \qquad \eta \to \infty \end{aligned} \tag{4.13}$$

If (4.11) is substituted into (4.12) and powers of η collected, there results a series of differential equations of the form

$$L_1 = B_1 U_1, \qquad L_2 = 2B_2 U_2, \qquad L_n = nB_n U_n - P_{n-2}, \qquad n \geq 3 \tag{4.14}$$

where L_n is the Legendre operator $L_n \equiv (1 - \xi^2)F_n'' - 2\xi F_n' + n(n-1)F_n$. The first two of these can be solved immediately, but the important point is that

$$P_m = \sum_{r=1}^{m} B_r \left\{ \frac{d}{d\xi} (1 - \xi^2) U_{r-1} F'_{m+1-r} + (m+1)(m+1-r) U_{r-1} F_{m+1-r} \right\} \tag{4.15}$$

so that F_n will depend only on lower orders.

Remembering that the Legendre functions of second kind $Q_n(\xi)$ have natural unwanted singularities at $\xi = \pm 1$ for all n, the desired homogeneous solutions of (4.14) are

$$\alpha_n P_{n-1}(\xi)$$

where the α_n are arbitrary constants. Furthermore, a particular solution of $L_n = nB_nU_n$ is $-B_nT_n$, and it is noteworthy that both contributions are polynomials of relatively simple structure in ξ. Now it can be shown by induction[3] that the equation $L_n = p_{n-2}$ has a particular solution q_{n-2} (say) which is a polynomial of degree $n-2$ when p_{n-2} is itself a polynomial — as is obvious for the first few terms in (4.14). In fact, a backward recursive algorithm to compute the coefficients of $q_{n-2}(\xi)$ from those of $p_{n-2}(\xi)$ can be set up which supplies both the computational mechanism and desired proof of existence at the same time (the important consideration is clearly whether or not a series assumption for $q_{n-2}(\xi)$ leads to termination).

On this basis, the complete sequence can be written

$$F_1 = \alpha_1 P_o(\xi) - B_1 T_1(\xi), \qquad F_2 = \alpha_2 P_1(\xi) - B_2 T_2(\xi)$$

$$F_n = \alpha_n P_{n-1}(\xi) - B_n T_n(\xi) - q_{n-2}(\xi), \qquad n > 2 \tag{4.16}$$

and the only remaining task is determination of the α_n constants from the boundary conditions.

4.4 Boundary Conditions

In 4.3 the general solution structure was described, but $n = 0$ is a special case which does not contain any constants. It can be shown that $F_o = \xi$ so that the leading term in the expression for ϕ is $\xi\eta$ and, therefore, $\phi \sim \xi\eta$ as $\eta \to \infty$ which means that (4.13) is satisfied.

With regard to the surface boundary condition (4.13), the constants α_n must be chosen. Consider for instance, the second-order approximation

$$\phi_2 = \eta\xi + [\alpha_1 - B_1 T_1]/\eta + [\alpha_2 \xi - B_2 T_2]/\eta^2$$

which can also be written in terms of $\cos\omega$ rather than the Chebyshev polynomials as

$$\phi_2 = \alpha_1/\eta + \left(\eta - \frac{B_1}{\eta} + \frac{\alpha_2}{\eta^2}\right)\cos\omega - \frac{B_2}{\eta^2}\cos 2\omega$$

giving

$$\left(\frac{\partial\phi_2}{\partial\eta}\right)_{n=1} = -\alpha_1 + (1 + B_1 - 2\alpha_2)\cos\omega - 2B_2\cos 2\omega$$

Obviously α_1 and α_2 cannot be chosen to make this vanish for all ω unless it happens that B_2 is zero. If $B_2 = 0$ then we choose $\alpha_1 = 0$, $\alpha_2 = (1 + B_1)/2$ to give

$$\phi_2 = \left(\eta - \frac{B_1}{\eta} + \frac{1 + B_1}{2\eta^2}\right)\cos\omega \qquad (4.17)$$

and if $B_2 \neq 0$ then the term in $\cos 2\omega$ will not satisfy the boundary condition. Ellipsoids are governed by choice of B_1 in the range $(-1 \leq B_1 \leq 1)$ but (4.17) is not the solution for arbitrary ellipsoids even though the B_n $(n \geq 2)$ vanish for both. The only exact case for (4.17) is $B_1 = 0$ which generates a circular profile and gives

$$\phi_2 = \left(\eta - \frac{1}{2\eta^2}\right)\cos\omega$$

as the correct potential for a sphere. Successive approximations for true ellipsoids are obtained by taking more terms and, in fact, ϕ_6 has been worked out by hand, but this academic topic will not be pursued further here. More details can be obtained from ref. 3.

However, the procedure described above is quite general. If the series for ϕ is terminated at the η^{-n} level, then the B_n term will not satisfy the surface boundary condition. For all higher-order terms, the α_n are determined by a set of n-2 linear simultaneous equations readily solved by standard methods. Since the number of terms required for bodies of practical interest is far less than the number of points required to describe the surface shape, the solution of this system of equations is a trivial task by modern computing standards. Typical term and point numbers are illustrated by the examples given later.

4.5 Velocity Calculation

For engineering purposes the quantity of greatest interest is the surface velocity which is given by

$$Q_s = -\frac{\partial\phi_s/\partial\omega}{ds/d\omega} \tag{4.18}$$

where s is the arc length measured from the trailing edge. There is a need for some care in using this formula since it is clear from (4.4) that

$$\frac{ds}{d\omega} = \left|\frac{dz}{d\zeta}\right| = \left(2\sin\frac{\omega}{2}\right)^{1-\tau/\pi}|g| \tag{4.19}$$

which vanishes at the trailing edge ($\omega = 0$). However, it is also clear that ϕ can be expressed in the form

$$\phi = G_0(\eta) + G_1(\eta)\cos\omega + G_2(\eta)\cos 2\omega + \ldots$$

once the α_n constants have been found. Therefore,

$$\frac{\partial\phi}{\partial\omega} = -[G_1(\eta)\sin\omega + 2G_2(\eta)\sin 2\omega + \ldots]$$

so that a factor $\sin\omega$ can be extracted to give

$$\frac{\partial\phi}{\partial\omega} = -\sin\omega[G_1 + 2G_2U_1 + \ldots] = -\sin\omega G(\xi,\eta) \tag{4.20}$$

where the U_n are again Chebyshev polynomials of the second kind. Equation (4.20) shows that the $\sin\omega$ factor can be used to cancel the zero in the denominator of (4.18) with the final, computationally sound result

$$Q_s = \frac{[2\sin(\omega/2)]^{\tau/\pi}\cos(\omega/2)\,G(\xi,1)}{|g|} \tag{4.21}$$

On this basis, direct computation of velocity given either the shape itself or B_n coefficients is quite straightforward. The central operation is a subroutine which calculates the coefficients of the polynomial powers of each succeeding F_n by recurrence relations and the $p \rightleftharpoons q$ algorithm mentioned in §4.4. These programs are described in more detail later, however, it is worth describing at this point the somewhat different philosophy behind the use of this theory as a design tool.

The obvious iterative procedure starting from a given (desired) Q vs s as input, is to guess B_n coefficients and compute the axisymmetric part $\partial\phi_s/\partial\omega$ together with $ds/d\omega$. One then argues that $\partial\phi_s/\partial\omega$ is less sensitive to the coefficients and computes the new estimate of $ds/d\omega$ by the algorithm

$$\left(\frac{ds}{d\omega}\right)_{n+1} = -\frac{(\partial\phi_s/\partial\omega)_n}{Q_s}$$

where Q_s is the given velocity. It is then a standard procedure using the Fast Fourier Transform subroutine to calculate the a_n coefficients (see e.g. 3).

Unfortunately, the presence of the singular factor $(2\sin(\omega/2)^{\tau/\pi}$ in the velocity formula makes this computationally unacceptable except for cusped bodies $\tau = 0$, and even then the front stagnation region $\omega = \pi$ causes difficulties. Consequently a procedure based on the wholly non-singular, nonzero group

$$\chi = G/|g|$$

was devised and forms the basis of the programs discussed later. The underlying principle is the same. Let the input desired velocity be denoted by $\tilde{Q}_s$ and quantities derived from it likewise by $\tilde{\chi}$, etc., then the new algorithm is

$$|g|_{n+1} = \frac{G_n}{\tilde{\chi}} \tag{4.22}$$

This is put into effect by using the calculated arc length from a given set of coefficients to interpolate for $\tilde{\chi}$ as a function of ω by dividing out the singular factor from the given velocity. Since G_n is also known from the n-th level of coefficients, the new estimate for $|g|$ and hence the new coefficients can be calculated from (4.22).

4.6 Solution Procedure

The body and its associated velocity distribution are essentially described by NP+1 point values in the upper half plane, shown in fig. 2, and taken from the trailing edge as origin. However, it is NP, not NP+1,

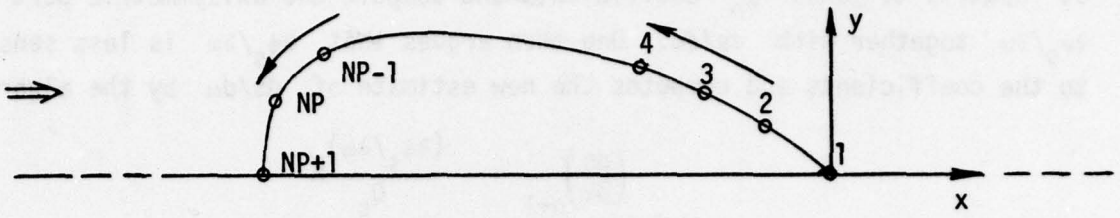


Figure 2. Body Geometry.

that is the crucial input parameter. There is a reason for this choice. Because of the use of a Fast Fourier Transform algorithm which uses a folding technique, NP must contain only the factors 2, 3 or 5.

Based on the provision of NP+1 data points, whether as (x,y)-values (direct mode), or as (Q,s)-values (design mode), the solution procedure depends upon a central subroutine which implements the conformal mapping, described in section 4.2, from a set of Fourier coefficients. These coefficients are computed internally from the given data.

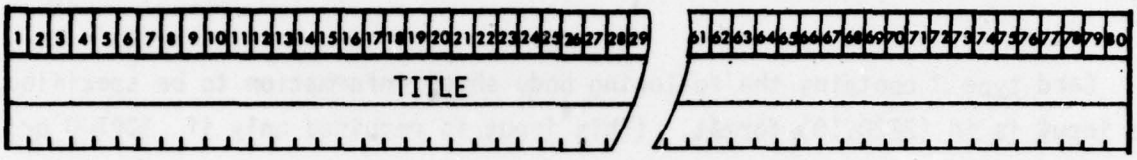
It is important to realize with regard to the design program that a given velocity does not necessarily design a closed body. The program outputs the body "closest" in a least squares (or rather Fourier) sense to having the desired velocity by compromising the overall level of maximum velocity whilst attempting to preserve the details. Thus, the designer is forced in turn to make compromises on his input levels and repeat the process.

This is an inescapable feature of design methods and has nothing to do with the structure of this particular program or even of axisymmetric as opposed to two-dimensional theory. For further discussion, see 3.

5.0 DESCRIPTION OF THE POTENTIAL-FLOW COMPUTER PROGRAM

5.1 Input

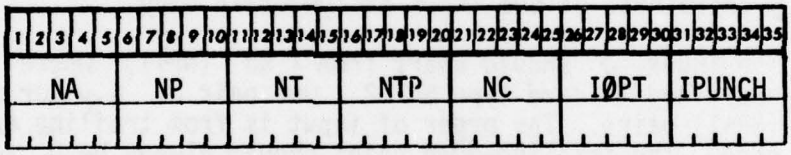
The input to the computer program consists of four types of cards. Card type 1 contains the title of the flow problem under consideration.



Load Sheet for Card 1

The title is input as an alphanumeric array with a format of (18A4).

Card type 2 requires the following control data to be specified. The input format is (7I5).



Load Sheet for Card 2

NA — Number of A_n coefficients to be used (for Fourier transforms) (default is NP).

NP — Number of surface elements on half of the body from trailing edge to leading edge.

NT — Number of terms to be used in the axisymmetric series (default is 21).

NTP — 0 or 1 (formerly used for trailing edge type specification, but currently not operative).

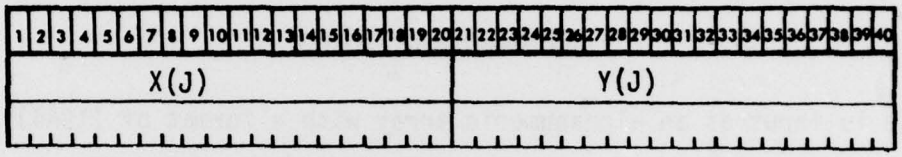
NC — Number of iterative cycles to be used in the axisymmetric inverse calculation (default is 20).

IØPT — Option for selective runs.
IØPT=0 program uses the body shape input (x,y data), calculates the direct axisymmetric velocity, then uses the computed velocity and normalized arc lengths to calculate the inverse shape (both direct and inverse calculations).

IØPT=1 program calculates only the direct flow solution from the input x,y data.
IØPT=2 program reads in the user's input velocity vs normalized arc-length data and computes the inverse shape only.

IPUNCH Option for punch output.
IPUNCH=1 program will generate the x,y data and the Q,S (velocity and normalized arc length) data. Two points per card.
IPUNCH=0 no punch output is desired.

Card type 3 contains the following body shape information to be specified. The input is in (2F20.10) format. (This input is required only if IØPT=0 or 1.)



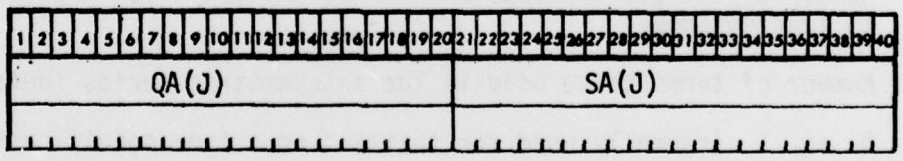
Load Sheet for Card 3

X(J) x-coordinate of the input axisymmetric body.

Y(J) y-coordinate of the input axisymmetric body.

Note: The index J should start from 1 to (NP+1) where NP is explained in card type No. 2. One pair of x,y per card up to (NP+1) pairs. The order of input is from trailing edge to leading edge. The trailing-edge point should always be 0, so that the x's go from 0 to negative value at leading edge. Only the upper half of the body is needed to be input as illustrated in Figure 2.

Card type 4 contains the velocity data to be specfiied. (This input is required only if IØPT=2.) The format for this input is 2F20.10.



Load Sheet for Card 4

QA(J) velocity at point J.

SA(J) normalized arc length at point J.

Note: One pair of QA vs SA per card. Subscript J starts at 1 and goes to (NP+1). There should be (NP+1) pair of (QA,SA) cards to be input. The order of input is from trailing edge to leading edge.

5.2 Output

The output from the inviscid potential-flow program first consists of a repeat of the input data used for the calculation. These are NA, the number of Fourier coefficients used; NTP, a parameter previously used to specify the trailing-edge type, but no longer used in the present code; NP, the number of body elements; NC, the number of iteration cycles specified (valid for inverse calculations only); NT, the number of terms in the axisymmetric expansion; IØPT, the parameter indicating direct or inverse mode. The specified body coordinates (direct case) or velocity and arc length (inverse case) are also given in tabular form.

For the direct calculation, the calculated output is presented in tabular form. The columnar headings are J, ØM(J), A(J), B(J), S(J), P(J), Q(J). These are:

J — designates the body point (last J=NP+1)

ØM(J) — angular displacement of body points measured from trailing edge ($0 \leq$ ØM(J) $\leq \pi$)

A(J) — x-location of body point

B(J) — y-location of body point

S(J) — normalized arc length of body point

P(J) — an internally used special axisymmetric derivative

Q(J) — computed value of the velocity

For the inverse calculation a running count of the iteration cycle and computed error is printed. If this value of the error falls below 10^{-5} the iterations are stopped and final results are printed. If this criterion is not satisfied, the iteration proceeds for NC cycles and the values after NC iterations are printed.

The final tabular results have the same headings in the inverse case as in the direct case, i.e., J, ØM(J), A(J), B(J), S(J), P(J), Q(J), but only J, ØM(J) and P(J), have the same meaning. The others are

A(J) — calculated x-location of body point

B(J) — calculated y-location of body point

S(J) normalized arc length of calculated body

Q(J) "least squares" velocity fit at body points, for converged shape (c.f. section 4.6).

5.3 Sample Calculations

Altogether, five bodies were used in the test cases described below. The first three, B1, B2 and B3, were characterized by having known Fourier coefficients for the mapping. Two more bodies, K1 and K2, were used, and these were chosen from boundary-layer design considerations. Therefore, as far as the theory described here is concerned, they were quite arbitrary, being defined only by (x,y) points. Figure 3 shows all five bodies.

Figure 4 shows the results of a direct calculation on bodies B1, B2, B3. The velocities are compared with the higher-order Neumann program[9] and it can be seen that the numbers of terms used in the present method were adequate to give excellent results.

In case there was a hidden bias toward the first three bodies just because they were originally derived from a conformal mapping, the direct solution procedure was applied to bodies K1 and K2. Figure 5 shows, once again, excellent results for the velocity distribution when compared with higher-order Neumann. Note that because these were thought to be harder cases (e.g., K1 has a flat portion as can be seen from Figure 5, and this is a poorly convergent feature) more terms were used (NA=21). Note also that K1 and K2 have nonintegral values of τ/π.

Finally, Figure 6 shows the results of using the program in the inverse (design) mode. Only the harder cases, K1 and K2, were used and it was expected that the original shapes should be returned. As can be seen in the figure, they were.

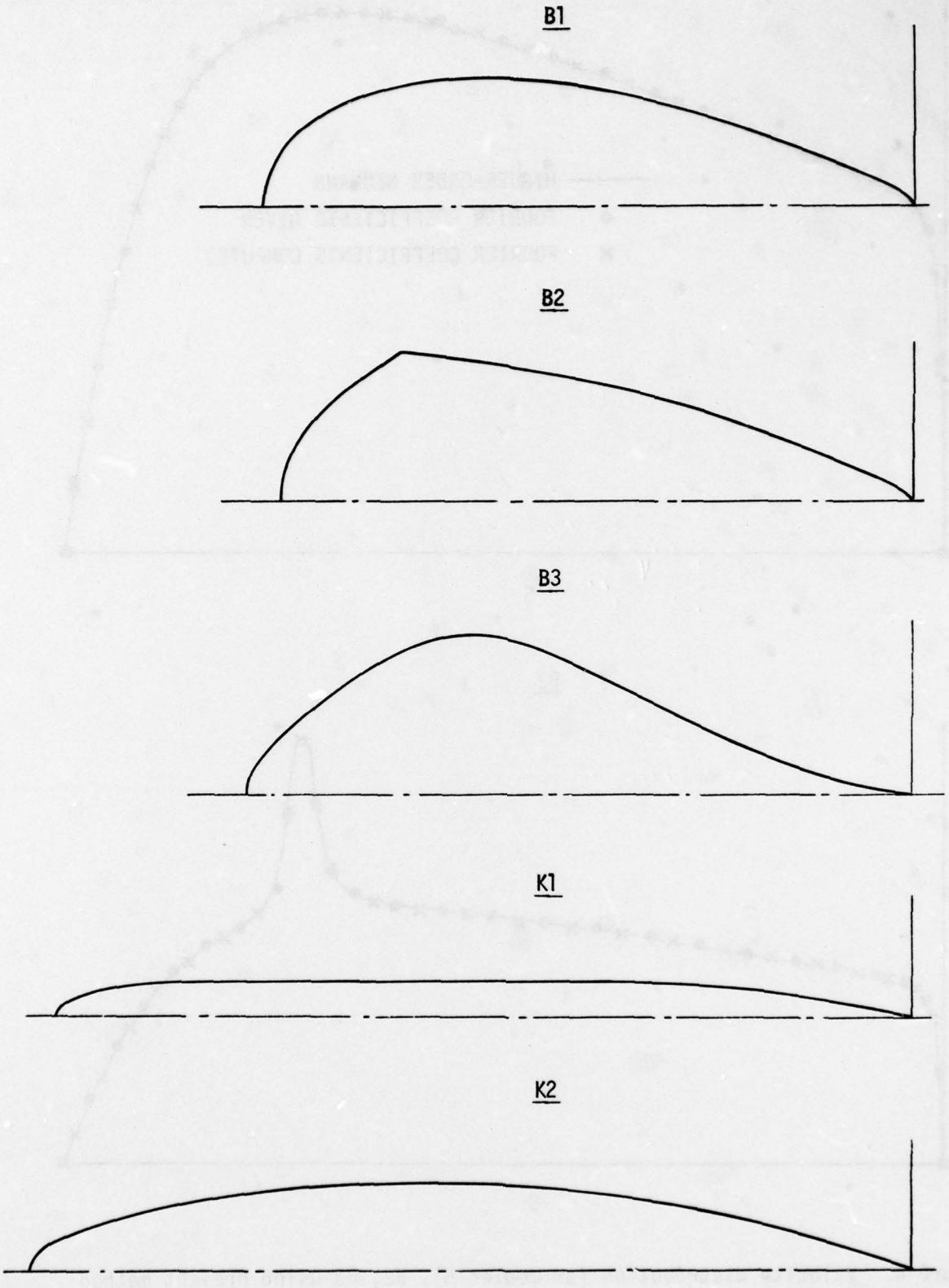


Figure 3. The five test bodies.

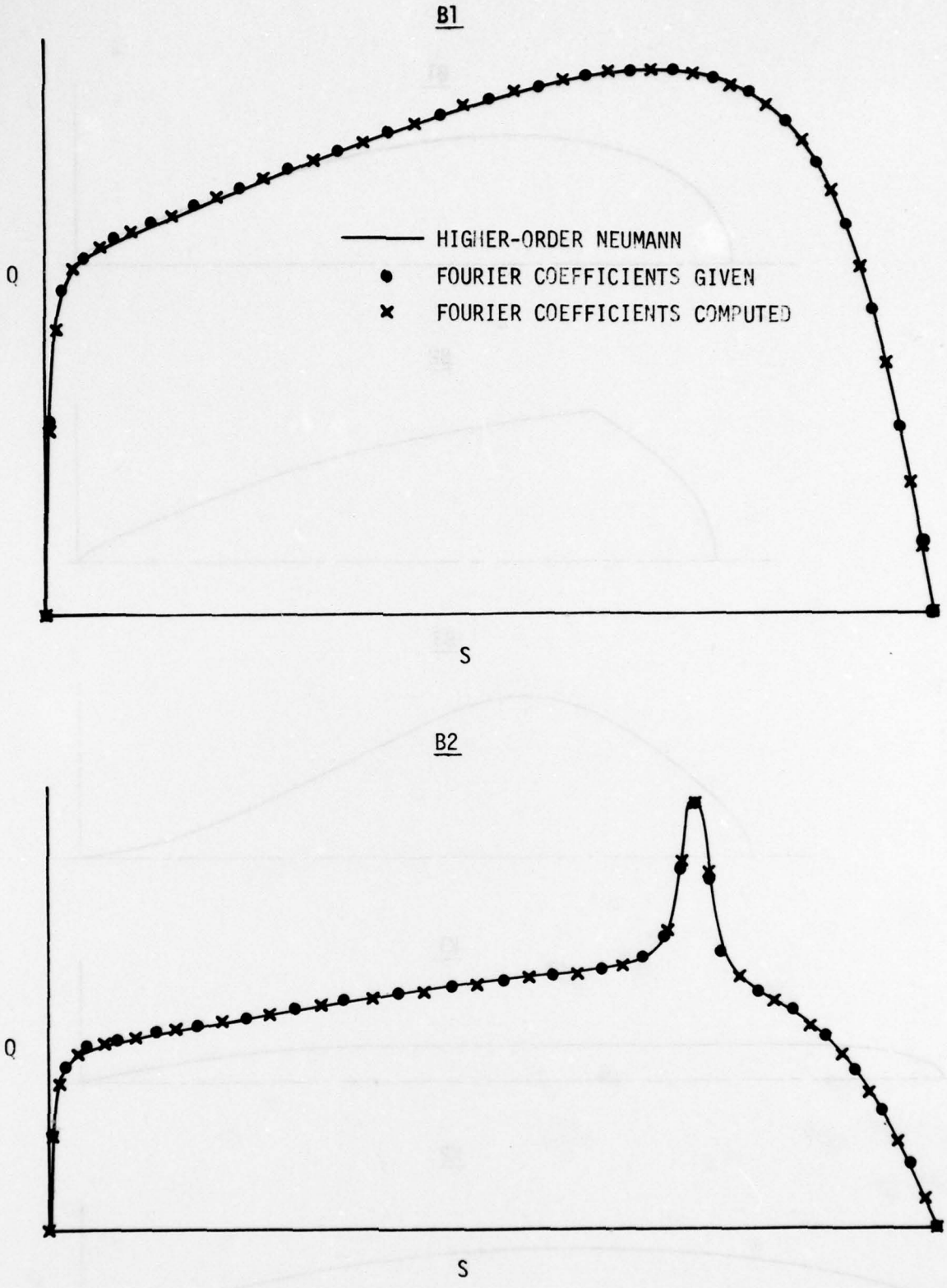


Figure 4. Velocity distribution for bodies B1, B2, B3 using present method and higher-order Neumann

B3

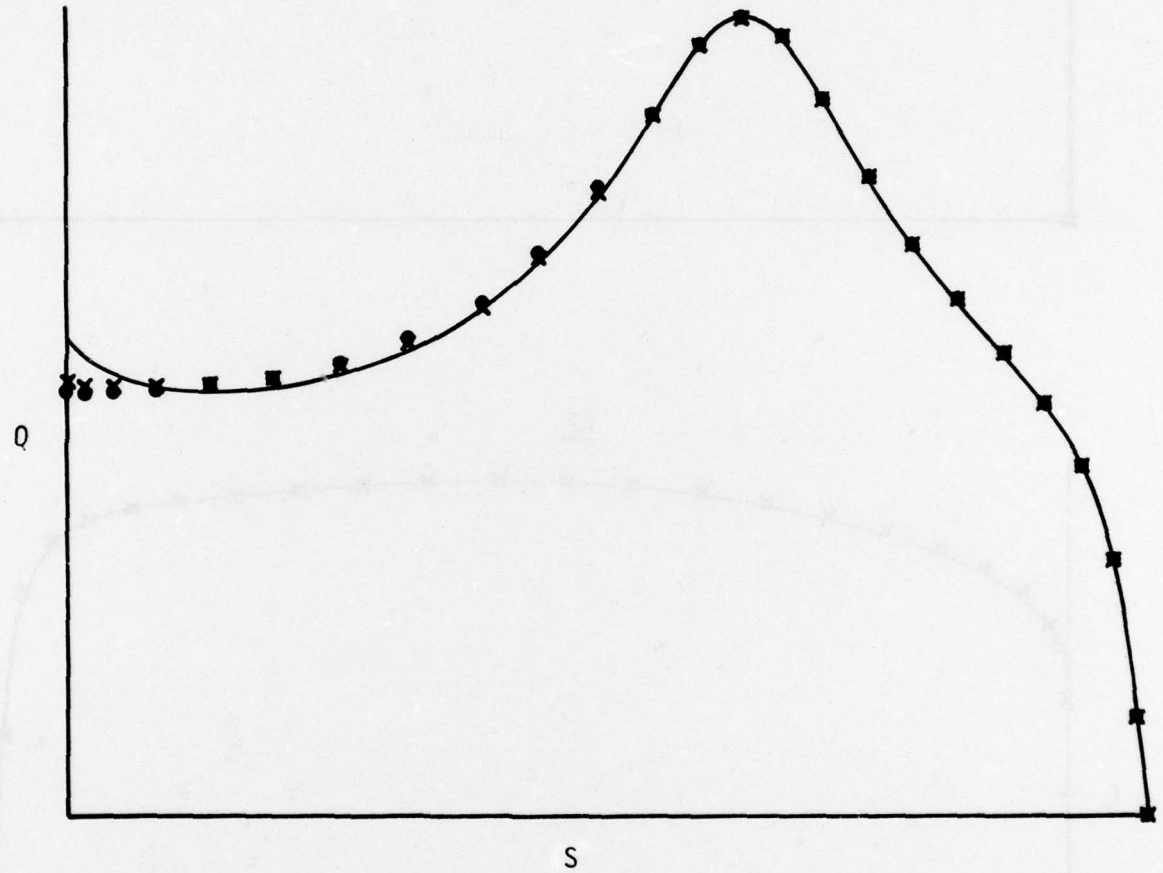


Figure 4. Continued

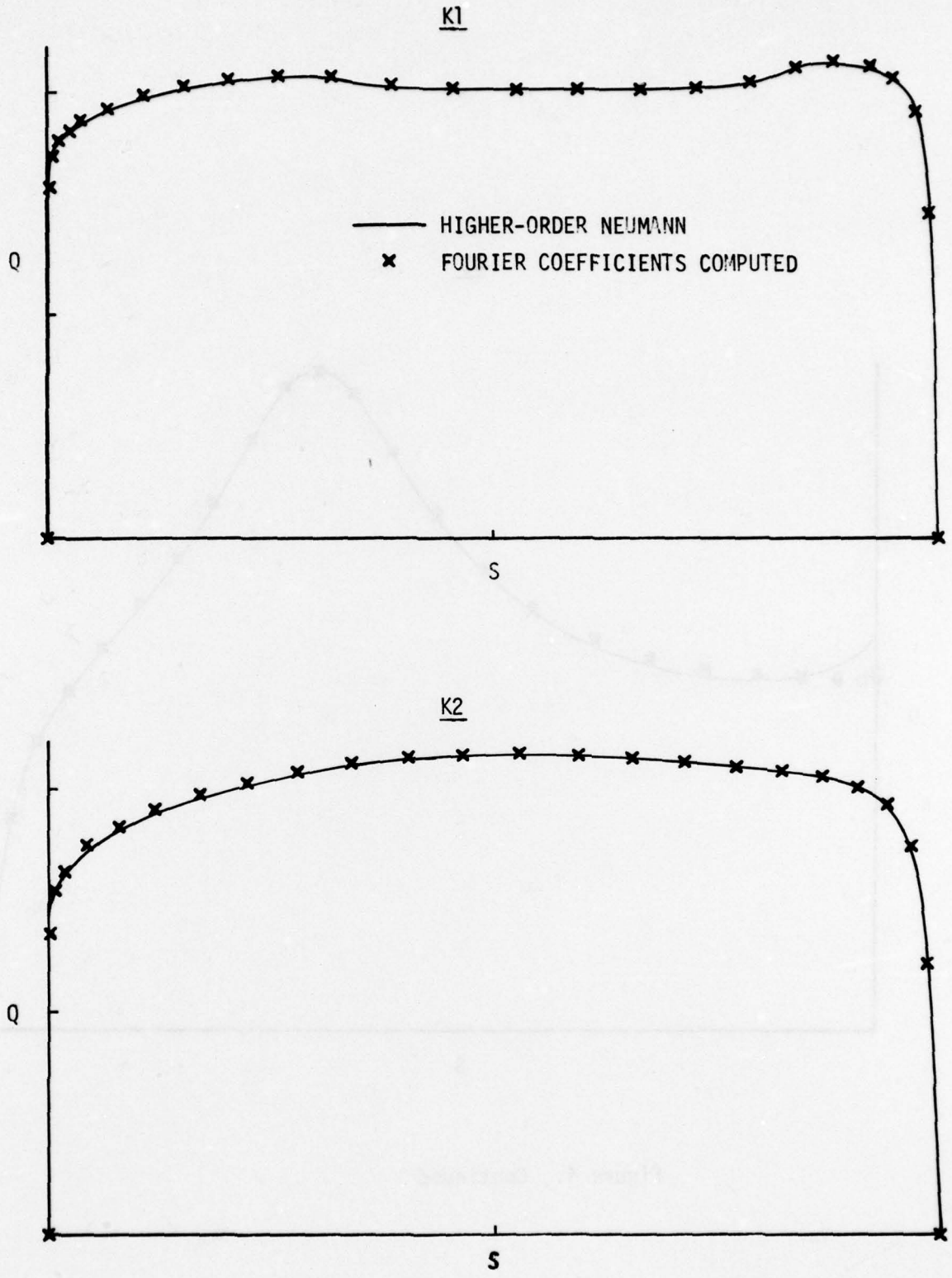


Figure 5. Velocity distribution for bodies K1, K2 using present method and higher-order Neumann.

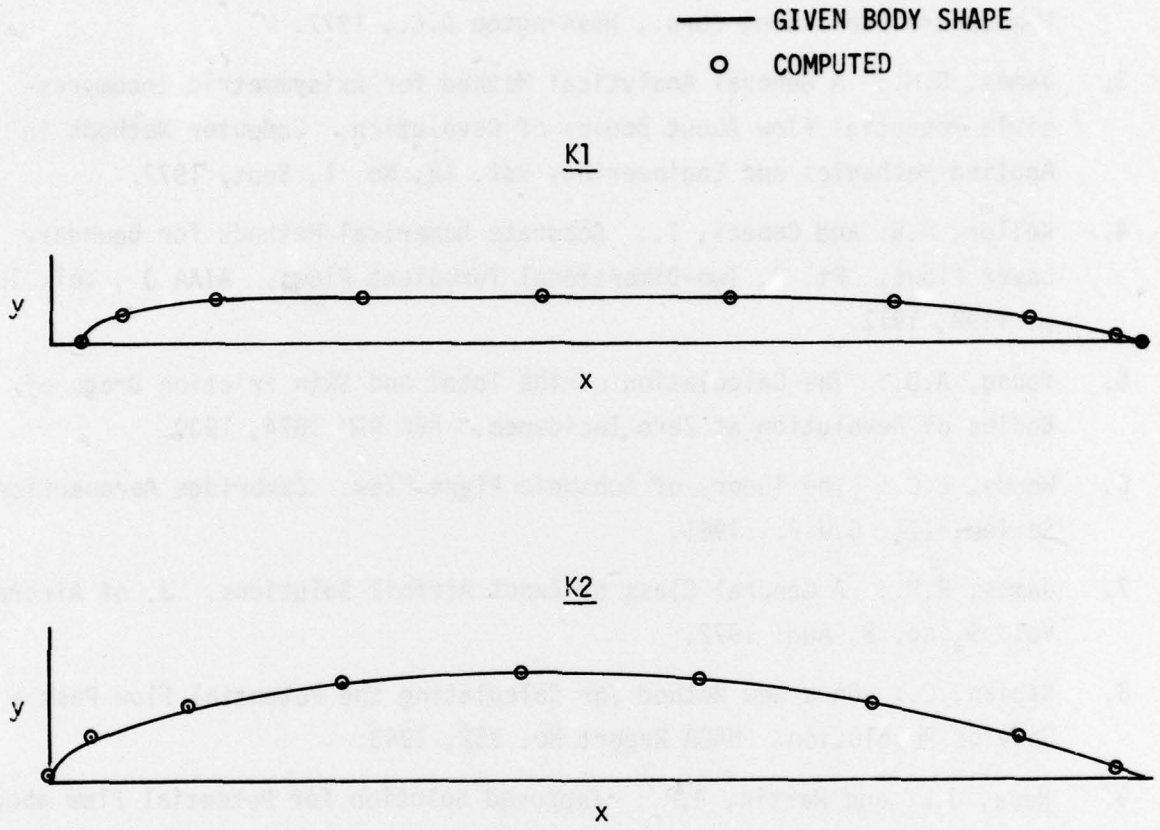


Figure 6. Computed body shapes for K1 and K2 using the (Q,S) inputs from figure 5.

6.0 REFERENCES

1. Cebeci, T. and Smith, A.M.O.: Analysis of Turbulent Boundary Layers. Academic Press, New York, 1974.

2. Cebeci, T. and Bradshaw, P.: Momentum Transfer in Boundary Layers. Hemisphere Publishing Corp., Washington D.C., 1977.

3. James, R.M.: A General Analytical Method for Axisymmetric Incompressible Potential Flow About Bodies of Revolution. Computer Methods in Applied Mechanics and Engineering. Vol. 12, No. 1, Sept. 1977.

4. Keller, H.B. and Cebeci, T.: Accurate Numerical Methods for Boundary Layer Flows. Pt. 2, Two-Dimensional Turbulent Flows. AIAA J., Vol. 10, p. 1193, 1972.

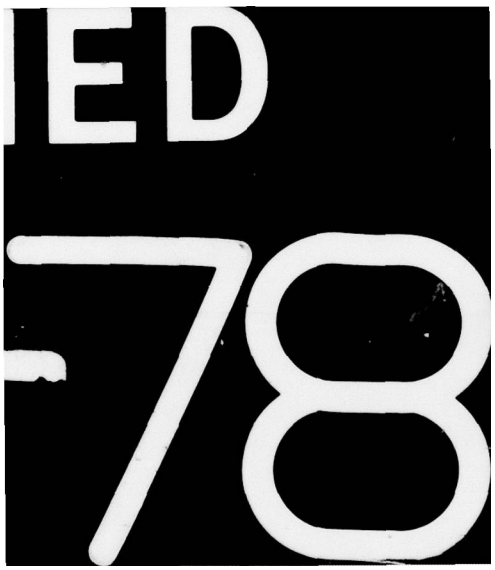
5. Young, A.D.: The Calculation of the Total and Skin Friction Drags of Bodies of Revolution at Zero Incidence. ARC R&M 1874, 1939.

6. Woods, L.C.: The Theory of Subsonic Plane Flow. Cambridge Aeronautical Series, III, C.U.P., 1961.

7. James, R.M.: A General Class of Exact Airfoil Solutions. J. of Aircraft, Vol. 9, No. 8, Aug. 1972.

8. Kaplan, C.: On a New Method for Calculating the Potential Flow Past a Body of Revolution. NACA Report No. 752, 1943.

9. Hess, J.L. and Martin, R.P.: Improved Solution for Potential Flow about Arbitrary Axisymmetric Bodies by the Use of a Higher-Order Surface Source Method. Part I. Theory and Results. NASA CR 134694, McDonnell Douglas Report No. MDC J6627-01, July 1974.


ED
78